Food Hydrocolloids 119 (2021) 106880

Contents lists available at ScienceDirect

Food Hydrocolloids

journal homepage: www.elsevier.com/locate/foodhyd

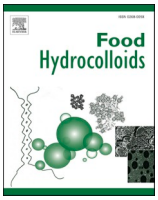

Mechanisms controlling wheat starch gelatinization and pasting behaviour in presence of sugars and sugar replacers: Role of hydrogen bonding and plasticizer molar volume

Stefano Renzetti *, Irene A.F. van den Hoek, Ruud G.M. van der Sman

Agrotechnology and Food Sciences Group, Wageningen University & Research, Wageningen, the Netherlands

ARTICLE INFO

Keywords:
Starch
Gelatinization
Swelling
Hydrogen bonding
Sugars
Fibres

ABSTRACT

The effect of sugars and sugar replacers (i.e. plasticizers) on the gelatinization and pasting behaviour of wheat starch was studied. The intrinsic properties of the plasticizers, i.e. the molar volume density of effective hydroxyl groups $N_{OH,s}/v_s$, and the volumetric density of hydrogen bonds in the sugar solutions treated as a single solvent, i.e. $\Phi_{w,eff}$, were proposed as factors controlling swelling (i.e. pasting) and gelatinization behaviour. Different classes of plasticizers were used including sugars, polyols, amino acids, soluble fibres such as oligofructoses, and mixtures thereof. The onset, peak and end temperature of starch gelatinization obtained by differential scanning calorimetry could be well described by $\Phi_{w,eff}$ for all solutions, following predictions from an adapted Flory-Huggins model for polymer melting. The multiple transitions involved in starch gelatinization could be well related to different ranges of $\Phi_{w,eff}$ following a side chain liquid crystalline model for starch. Deviations from the model predictions were observed mainly for T_{onset} in conditions of intermediate and excess solvent with high sugar concentrations (50% w/w). In such conditions phase separation likely occurs, increasing the effective starch concentration and consequently gelatinization temperatures. Pasting behaviour related to swelling, i.e. peak viscosity, was found to be a sigmoidal Fermi function of $N_{OH,s}/v_s$ of the plasticizers. Plasticizers with high $N_{OH,s}/v_s$ enhanced swelling compared to water while those with low $N_{OH,s}/v_s$ had an inhibition effect. Overall, a comprehensive mechanism of starch plasticization, swelling and melting is proposed. Swelling associated with solvent ingress and helix-helix dissociation is affected by kinetic factors related to size and viscosity of the plasticizers (both described by $N_{OH,s}/v_s$) and by thermodynamic factors related to sugar partitioning and H-bonding ability (both related to $\Phi_{w,eff}$). Melting of crystalline domains associated to helix-coil transition is controlled by thermodynamics, based on solvent H-bonding ability $\Phi_{w,eff}$.

1. Introduction

Starch is a macro-constituent of many foods and its properties and interactions with other constituents (e.g. water, sugars and polysaccharides) during food processing are particularly of interest to the food industry and for human nutrition. Starch occurs naturally as insoluble, semi-crystalline granules, made up of amylose and amylopectin (Tester, Karkalas, & Qi, 2004; Copeland, Blazek, Salman, & Tang, 2009). These biopolymers are structurally organized in blocklets having a lamellar structure of alternating crystalline and amorphous layers (Donald, 2004; Donald, Kato, Perry, & Waigh, 2001; Pérez, Baldwin, & Gallant, 2009). The crystalline lamellae is constituted by the double helices of the amylopectin molecules arranged into 'clusters'. The starch granules are the result of multiple concentric growth rings resulting from these blocklets (Tester et al., 2004; Copeland et al., 2009; Pérez et al., 2009; Bertoft, 2018).

Under specific temperature and moisture conditions, starch undergoes a phase transition named gelatinization, which is the irreversible disruption of the native, semi-crystalline organization of the starch granule into a polymer solution in the rubbery state. This process actually involves multiple transitions, which can be described using the framework derived for synthetic side-chain liquid crystalline polymers (Donald, 2001; Waigh, Gidley, Komanshek, & Donald, 2000). First water enters the amorphous growth rings and the starch granule swells (Jenkins & Donald, 1998). The amorphous background is where all the initial swelling is concentrated. Only once a large amount of swelling has

* Corresponding author.
E-mail address: stefano.renzetti@wur.nl (S. Renzetti).

https://doi.org/10.1016/j.foodhyd.2021.106880
Received 10 January 2021; Received in revised form 5 April 2021; Accepted 30 April 2021
Available online 4 May 2021

occurred in the amorphous background there is sufficient stress imposed through connecting molecules from the amorphous to the crystalline regions, to start disrupting the crystals themselves. At this stage, helix-helix side chains dissociate (smectic to nematic/isotropic) followed by unwinding of the double helices via helix-coil transition (nematic/isotropic to gel) (Waigh et al., 2000). The latter process can be viewed as the main melting event during gelatinization, which occurs late in the gelatinization process.

The starch gelatinization detected by differently scanning calorimetry (DSC) is affected by water contents (Donovan, 1979). In excess water (>65% w/w) only one endotherm is observed, namely G endotherm, which represents gelatinization accompanied by the uptake of water (Donovan, 1979; Evans & Haisman, 1982; Steeneken & Woortman, 2009). Upon decreasing the water content between 35 and 65% two endotherms are observed, namely G and M endotherm. The M endotherm represents the melting of crystals (Donovan, 1979; Steeneken & Woortman, 2009). Decreasing the amount of water below 35%, only one endotherm is observed at high temperature (Donovan, 1979). The effects of hydration on the DSC traces is consistent with the side-chain liquid crystalline model proposed by (Waigh et al., 2000).

The gelatinization process is also coupled to changes in viscosity, often studied with a rapid visco analyser (RVA). In concentrated regime conditions of the RVA, starch granules cannot swell to their maximum because of space restrictions (Renzetti & Arendt, 2009; Renzetti, Courtin, Delcour, & Arendt, 2010). The increase in the volume fraction of granules leads to a closely packed condition of a starch paste. The peak viscosity recorded in the RVA corresponds to the point when the swelling of intact starch granules is at a maximum (Balet, Guelpa, Fox, & Manley, 2019). The maximum is followed by a decrease in paste viscosity, as the granules rupture and starch molecules are dispersed in the aqueous phase (Copeland et al., 2009).

The amorphous phase plays a significant role in the phase transition of granules during gelatinization. The endotherm G in DSC profiles of starch/water systems represents the energy change mainly associated with water absorption and granule swelling to its maximum with partial leaching of starch polymer molecules (Wang, Li, Yu, Copeland, & Wang, 2014; Wang, Zhang, Wang, & Copeland, 2016; Kovrlija & Rondeau-Mouro, 2017). Amylose leaching can be viewed as a kind of phase separation due to the incompatibility of the linear amylose and branched amylopectin polymers (Van Der Sman & Meinders, 2011; Yuryev, Nemirovskaya, & Maslova, 1995). The increase in viscosity during the cooling period of RVA tests indicates the tendency of the amylose to re-associate with decrease in temperature, thus contributing to set-back and final viscosity (Balet et al., 2019).

It is widely reported that sugars increase gelatinization temperature and affect the gelatinization enthalpy as well as swelling and pasting behavior (Perry & Donald, 2002; Kweon et al., 2016a,b; Evans & Haisman, 1982; Spies & Hoseney, 1982) ; Ahmad & Williams, 1999). Prevailing hypotheses on the underlying mechanisms were based on water activity (Evans & Haisman, 1982; Spies & Hoseney, 1982), glass transition temperatures (Slade & Levine, 1988), and H-bonding interactions between starch and sugars (Spies & Hoseney, 1982; Nashed & Sopade, 2003; Baek, Yoo, & Lim, 2004). However, none of these hypothesis can fully explain starch gelatinization behaviour in presence of sugars, neither swelling/pasting behaviour (Allan, Rajwa, & Mauer, 2018).

A major shortcoming of most from the reported studies is that they considered water and sugars separately, as if the nature of the specific H-bonding interactions would differ (Perry & Donald, 2002). and (Tan, Wee, Sopade, & Halley, 2004) suggested that any solvent with hydrogen bonds is able to gelatinize starch and that the intrinsic properties of the solution as a whole are of importance in determining gelatinization behaviour. Recently (van der Sman, 2016), suggested that mixtures of sugars and polyols in water can be treated as a single solvent when described in terms of an effective solvent volume fraction, i.e. $\Phi_{w,eff}$. The $\Phi_{w,eff}$ accounts for the volumetric density of hydrogen bonding sites available in the solution for interaction with biopolymers such as proteins and starches. Following on a thermodynamic approach based on Flory-Huggins (FH) theory for biopolymer melting, $\Phi_{w,eff}$ has been successfully used to describe the phase transitions of biopolymers such as protein denaturation and starch gelatinization (van der Sman, 2016; Renzetti, van den Hoek, & van der Sman, 2020). Nevertheless, the mechanims by which sugars control starch gelatinization are still unclear as non-equilibrium (kinetic) processes such as diffusion of solvent into the starch granules and swelling of granules are relevant aspects which have not been accounted for in these studies. Recent studies have looked at gelatinization in presence of sugars in excess solvent only (Allan et al., 2018; van der Sman & Mauer, 2019), while lower hydration conditions have not been investigated. The effect of sugars on gelatinization as determined by DSC and on swelling and pasting as determined by RVA have not been coupled yet. Furthermore, phase separation between a starch-rich phase and a sugar-solution phase can occur at sugar concentrations above 15% (dry matter basis) (Roudaut & Wallecan, 2015; Kawai & Hagura, 2012) and it can affect biopolymers melting, as observed for denaturation of egg white proteins in sugar solutions (Renzetti et al., 2020). The latter study suggested that phase separation occurs in conditions of intermediate to excess solvent, (i.e. $\Phi_{w,eff} > 0.3$). Drivers for phase separation were sugar concentration and the molar volume density of effective hydroxyl groups, i.e. $N_{OH,s}/v_s$, of the sugars or sugar replacing mixtures. The $N_{OH,s}/v_s$ is an intrinsic property of the plasticizer, which represents the number of H-bonding sites effectively available for intermolecular interactions within the molar volume of a sugar.

Based on this background, the objective of this study was to determine whether the solvent properties of sugar and sugar replacer solutions, i.e. $\Phi_{w,eff}$, and the intrinsic properties of the plasticizers, i.e. $N_{OH,s}/v_s$, can describe the gelatinization and swelling behaviour of wheat starch. For these purposes, gelatinization was studied by DSC at various conditions of hydration (i.e. starch:solvent ratio's). An adapted FH theory was applied to test the validity of $\Phi_{w,eff}$ in conditions of both excess as well as intermediate and limited solvent. Swelling of starch in sugar solution was studied by means of RVA. Both gelatinization and pasting behaviour were studied in complex solvent systems ranging from binary to quaternary water/plasticizers mixtures and combined different classes of compounds, at concentrations up to 50%. Among the sugar replacers, amino acids such as L-proline and glycine were included as novel alternative plasticizers (van der Sman, van den Hoek, & Renzetti, 2020) as compared to polyols and soluble fiber, similarly to our recent study on egg white denaturation (Renzetti et al., 2020).

2. Theoretical background for quantitative description of starch gelatinization

2.1. Effective number of hydroxyl groups available for intermolecular hydrogen bonding

As recently described (van der Sman, 2013), the dry T_g of carbohydrates and polyols is controlled by the effective number of hydroxyl groups, $N_{OH,s}$, available for intermolecular hydrogen bonding. $N_{OH,s}$ differs from the total number of hydroxyl groups in a molecule as it is corrected for intramolecular hydrogen bond interactions due to stereochemistry (Pawlus, Grzybowski, Paluch, & Wlodarczyk, 2012). For classes of molecules such as sugars, polyols and sugar oligomers, $N_{OH,s}$ is inversely proportional to the glass transition temperature of the pure compound via:

$$\frac{1}{2}\frac{T_g - T_{g,w}}{T_g^{\infty} - T_{g,w}} = \left(\frac{1}{2} - \frac{N}{N_{OH,s}}\right) \quad (1)$$

where T_g is the glass transition temperature of the pure compound, $T_{g,w}$ is the glass transition temperature of pure water, T_g^{∞} is the glass transition temperature of a compound of infinite size from a particular class

of materials (i.e. $T_g^{\infty} = 450$ K for glucose-oligomers, 448 K for fructose oligomers and 339 K for polyols) and $\frac{N}{N_{OH,s}}$ is the inverse of the number of hydroxyl groups per molecule. The dry T_g of the plasticizers can be used to calculate $N_{OH,s}$ as recently reported for sugars and polyols (van der Sman & Mauer, 2019). For glycine and proline the dry $T_{g,s}$ are estimated 220 and 250 K, respectively (van der Sman et al., 2020).

For oligosaccharides, the dry $T_{g,s}$ can be computed from their M_n following on the Fox-Flory equation (Fox & Flory, 1950):

$$T_g = T_{g,\infty} - \frac{C}{M_n} \tag{2}$$

with $T_{g,\infty}$being the T_g at infinite molecular weight, M_n the number averaged molecular weight and C a constant. The constant C for oligofructoses was reported as 75 kDa (Mensink, Frijlink, Van Der Voort Maarschalk, & Hinrichs, 2015). This approach has been recently validated by correlating the computed T_g and the effective number of hydrogen bonds in solutions of soluble fibres solutions to viscosity measurements (van der Sman & Mauer, 2019; Renzetti et al., 2020).

Equation (1) was used to obtain the $N_{OH,s}$ of sugars and sugar replacers in this study, similarly to what recently reported (van der Sman, 2016; van der Sman and Mauer, 2019; Renzetti et al., 2020). For soluble fibres, i.e. oligofructoses, equation (2) was used to derive the dry $T_{g,}s$.

From the $N_{OH,s}$ of sugars and sugar replacers, the number of H-bonding sites effectively available within the molar volume of plasticizer for intermolecular interactions is obtained, i.e. $N_{OH,s}/v_s$, where v_s is the molar volume of the plasticizer. In presence of mixtures of plasticizers, $N_{OH,s}/v_s$ is computed from (Renzetti et al., 2020):

$$\left(\frac{N_{OH,s}}{v_s}\right)_{mixture} = \frac{\sum_i \Phi_s \frac{N_{OH,s}}{v_s}}{\sum_i \Phi_s} \tag{3}$$

where Φ_s is the volume fraction of each plasticizer in the mixture.

2.2. Quantitative description of starch gelatinization via Flory-Huggins theory for polymer melting extended with the volumetric density of the effective number of hydroxyl groups

According to the FH theory, the biopolymer melting temperature in a water solution can be described as function of the volume fraction of water (Φ_{water}) present in the system, following the equation (van der Sman, 2016):

$$\frac{1}{T_m} - \frac{1}{T_m^{\circ}} = \frac{R}{\Delta H_U}\frac{v_U}{v_W}\left[\Phi_{water} - \chi\Phi_{water}^2\right] \tag{4}$$

where T_m (K) is the melting temperature of the biopolymer in the system under consideration, T_m° (K) the melting temperature of the dry biopolymer, ΔH_U (kJ/mol) is the melting enthalpy per mole of the repeat unit of the biopolymer, v_U is the molar volume of the biopolymer repeat unit, v_w is the molar volume of water, χ is the FH solvent-biopolymer interaction parameter and R is the universal gas constant. It should be noted that in the FH theory, the crystalline phase of biopolymers do not absorb water. The volume fraction of the biopolymer in the rubbery state is computed based on its degree of crystallinity ξ (Van Der Sman & Meinders, 2011).

For describing the gelatinization behavior of starch in the sugars and sugar replacers solutions, the volume fraction of water Φ_{water} in equation (4) is better replaced by the effective volume fraction of the solvent, $\Phi_{w,eff}$, comprising the mixture of water and all dissolved sugars according to (van der Sman, 2016):

$$\Phi_{w,eff} = \Phi_w + \sum_i \Phi_{s,i}\frac{N_{OH,s}v_w}{N_{OH,w}v_s} \tag{5}$$

where Φ_w is the volume fraction of water, $\Phi_{s,i}$ that of the plasticizer and $v_w$and v_s are the molar volume of water and plasticizer, respectively, obtained from the ratio of their molar weight over their mass density. The $N_{OH,s}/v_s$ represents the number of H-bonding sites effectively available within the molar volume of a sugar for intermolecular interactions. For the mixtures under investigation, it holds that $\Phi_w + \Phi_s = 1 - \Phi_p$, with $\Phi_p$the volume fraction of starch. The volume fraction of components in the mixtures is computed from the mass fraction using the mass density ρ_i of each ingredient, as previously reported (Renzetti et al., 2020).

Following on the description of $\Phi_{w,eff}$, the FH equation (3) is re-written as (van der Sman, 2016):

$$\frac{1}{T_m} - \frac{1}{T_m^{\circ}} = \frac{R}{\Delta H_U}\frac{v_U}{v_W}\left[\Phi_{w,eff} - \chi_{eff}\cdot\Phi_{w,eff}^2\right] \tag{6}$$

with the effective interaction parameter equal to (van der Sman, 2016):

$$\chi_{eff} = \chi_0 + (\chi_1 - \chi_0)\left(1 - \Phi_{w,eff}^2\right) \tag{7}$$

χ_0 is the interaction parameter of the hydrated biopolymer and equal to 0.5, while χ_1 that of the dry biopolymer, independently of temperature (van der Sman, 2016).

3. Materials and methods

3.1. Materials

Wheat starch (5% moisture) was purchased from Sigma-Aldrich (St. Louis, MO, US). Eleven different plasticizers among sugars, polyols, amino acids and fructo-oligosaccharides were used in the study. Glucose, sucrose, xylitol, proline and glycine were from Sigma-Aldrich (St. Louis, MO, US); five different fructo-oligosaccharides were used: Frutalose OFP (OFP), Frutafit CLR (CLR), Frutafit IQ (IQ) and Frutafit TEX (TEX) provided by Sensus (Roosendaal, The Netehrlands) and Actilight (FOS) from Tereos (Marckolsheim, France); the polydextrose (PDX) Litesse Ultra was supplied by DuPont (Wilmington, Delaware, US). The average molecular weight of the fructo-oligosaccharides was preliminarily determined from the degree of polymerization of the constituent polysaccharides as recently described (Renzetti et al., 2020). The fructo-oligosaccharides varied in molecular weight, with FOS being 605 g/mol ($M_n = 564$), OFP 725 g/mol ($M_n = 626$), CLR 1769 g/mol ($M_n = 878$), IQ 2184 g/mol ($M_n = 982$), TEX 3877 g/mol ($M_n = 2813$), based on DP analysis provided by the suppliers.

3.2. Methods

3.2.1. Starch gelatinization in water solution and in solutions of sugar and sugar replacers

Starch gelatinization was first studied as function of water content by preparing different ratio's between starch and water. In particular, starch-water mixtures with water mass fractions ranging from 0.1 to 0.9 (w/w) with incremental steps of 0.1 and of 0.05 (w/w) were studied.

Then, thirty-one different solutions were prepared using single compounds as well as mixtures of two and three plasticizers in water. The twenty-two solutions comprising single compounds are listed in Table 1. The nine solutions comprising mixtures of sucrose, xylitol and oligofructoses are listed in Table 2. Distilled water was used in all preparations. Solutions were slightly heated (up to ≈ 60 °C) to ensure complete dissolution. Starch gelatinization was studied in the sugar and sugar replacer solutions listed in Table 1 by using the same range of solvent mass fractions (0.1–0.9) as for the study with water. Solvent mass fractions of 0.7 and 0.5 were studied for the solution with FOS, CLR, PDX, IQ, TEX and for the ternary and quaternary mixtures listed in Table 2, except for solution #9 which was studied for all ranges of solvent mass fractions.

DSC was used to determine the gelatinization behavior of starch in the different solutions. High volume hermetic stainless steel cups were

Table 1
Compositions of sugars and sugar replacers in water used for the starch gelatinization experiments.

Plasticizers	Concentrations (%, w/w)
Sugars	
Glucose	15, 30, 50
Sucrose	15, 30, 50
Polyols	
Xylitol	30
Soluble fibres	
Frutafit OFP (OFP)	15, 30, 50
Polydextrose Litesse Ultra (PDX)	30, 50
FOS Actilight (FOS)	30
Frutafit CLR (CLR)	30
Frutafit IQ (IQ)	15, 30
Frutafit TEX (TEX)	10, 30
Amino acids	
Glycine	15
Proline	15, 30, 50

Table 2
Compositions (%, w/w) of ternary and quaternary mixtures of sugars and sugar replacers in water.

#	water	sucrose	xylitol	FOS Actilight	Frutalose OFP	Frutafit IQ
1	70	22.5	1.8	5.7		
2	70	15	3.6	11.4		
3	70		7.2	22.8		
4	70	22.5	7.5			
5	70	15	15			
6	70	22.5		7.5		
7	70	15		15		
8	70				15	15
9	70		7.2		22.8	

filled first with the starch (3 mg–24 mg on dry matter, depending on targeted concentration) and then the solution was added. Cups were closed and stored overnight at room temperature to allow full hydration of the starch. Tests conducted to assess the effect of hydration time on gelatinization profile indicated full hydration at the conditions used in this study. After hydration, samples were then analyzed in a DSC Q200 (TA Instruments, New Castle, USA) by first equilibrating at −10 °C for 5 min and then by heating up at a rate of 5 °C/min to a temperature of: 160 °C for starch concentrations between 10 and 60%, 180 °C for 70% starch and 230 °C for starch concentrations of 80% and below. The onset of starch gelatinization (T_{onset}), peak temperature (T_{peak}) and end temperature (T_{end}) were determined using the analysis tools available in the Universal Analysis software (TA instruments, New Castle, USA). Experiments were performed in triplicates.

The starch gelatinization data (T_{onset}, T_{peak} and T_{end}) derived from the DSC measurements were tested with the extended FH theory to check the validity of $\Phi_{w,eff}$ for various sugars, sugars replacers and mixtures thereof.

3.2.2. Starch pasting behaviour in water and in solutions of sugar and sugar replacers

A Rapid Visco Analyser (Newport Scientific Pvt. Ltd., Warriewood, Australia) was used to determine the pasting properties of wheat starch in different solutions. Starch suspensions of 8% dry matter (dm) in different solutions were prepared for a total weight of 25.0 g. Samples were then subjected to the following time–temperature profile: hold at 50 °C for 1 min (mixing for 10 s at 960 RPM and then decrease to 160 RPM for the rest of the measurement), increase to 95 °C over 3 min 42 s, hold at 95 °C for 2 min 30 s, decrease to 50 °C over 3 min 48 s and hold at 50 °C for 5 min. The viscosity was expressed as cP.

Solutions of 10, 20, 30 and 40% (w/w) were studied for glucose, sucrose, maltitol, xylitol, proline, FOS, a xylitol-FOS (1:3.2) mixture and a sucrose-FOS (1:1) mixture. Solutions of 10, 20 and 30% TEX and 30% IQ were also studied. Furthermore, solutions #1–7 in Table 2 were also tested.

Analyses were performed in duplicate, with a relative difference of <1% for all samples. Sample moisture was determined using the air-oven method (Approved method 44-15 A, AACC International 2000).

3.2.3. Statistical analyses

The data were analyzed using statistical functions in Rstudio (RStudio, Inc., Boston, MA, USA). All model parameters were computed using non-linear least squares. Significant differences were determined by one-way ANOVA, with a comparison of mean values using the Tukey test ($\alpha = 0.05$).

4. Results

4.1. Starch gelatinization in water solutions

Starch gelatinization was studied at different levels of hydration with water mass fractions (wmf) ranging from 0.05 to 0.9, resulting in different DSC profiles (Fig. 1A). In diluted solutions (wmf > 0.5) one starch melting endotherm, i.e. G, could be clearly detected with T_{peak} at about 60 °C, with a smaller peak around 100 °C associated to the melting of the amylose-lipid complex. The latter was confirmed by a second scan of the starch sample (data not shown), showing the re-appearance of the complex (Kugimiya & Donovan, 1981). At wmf of 0.4 and 0.3, the DSC thermogram became more complex, with a new peak, i.e. M, appearing above 60 °C (Fig. 1A and B, for wmf = 0.3). At wmf of 0.2 and below, one starch melting peak was detected at temperatures above 140 °C.

The interpretation of the DSC traces at intermediate and low moisture contents is critical for the definition of gelatinization behaviour, i.e. T_{onset}, T_{peak} and T_{end}. The coupling between the double helices and the backbone in the amylopectin structure through the flexible spacers (i.e. the amorphous phase) is affected dramatically by the water content (Steeneken & Woortman, 2009). The two stage process proposed by (Waigh et al., 2000) was used for interpretation of the DSC traces in this study.

At high water contents (wmf > 0.5), the amylopectin double helices can only unwind if they are dissociated from their crystallites. Hence, as the temperature is increased an endotherm occurs only as the helices dissociate side-by- side (slow), and the helix-coil transition happens as an immediate consequence of this step (fast). The endotherms associated to these transitions merge together into the G peak in the DSC traces, which occurs at the point of complete loss of helical ordering (Fig. 1B wmf = 0.8). In this conditions, T_{onset}, T_{peak} and T_{end} were derived from the G endotherm.

At wmf between 0.5 and 0.2, as the system is heated the thermal energy eventually becomes sufficient to increase the mobility of the amylopectin double helices side-by-side resulting in a smectic to isotropic phase change (denoted G in Fig. 1B with wmf = 0.3). Adding yet further heat, the helices unwind through their extremely cooperative transition and birefringence of the granule is lost (denoted M). Hence, the helix–coil transition (M) occurs at higher temperatures than the smectic to isotropic one (G), resulting in two main endotherms in the DSC traces. In this conditions, the onset of the G endotherm was defined as T_{onset} while T_{peak} and T_{end} of starch gelatinization were derived from the M endotherm (Fig. 1B with wmf = 0.3).

In very low water contents (wmf<0.2), a direct helix to coil phase change occurs from the crystalline state at elevated temperatures (Waigh et al., 2000). The mobility of the backbone and spacers is not sufficient to stabilize a mobile isotropic phase, and only a single endotherm occurs in the DSC trace (wmf 0.1 and 0.05 in Fig. 1A). In this conditions, T_{onset}, T_{peak} and T_{end} were derived from this single

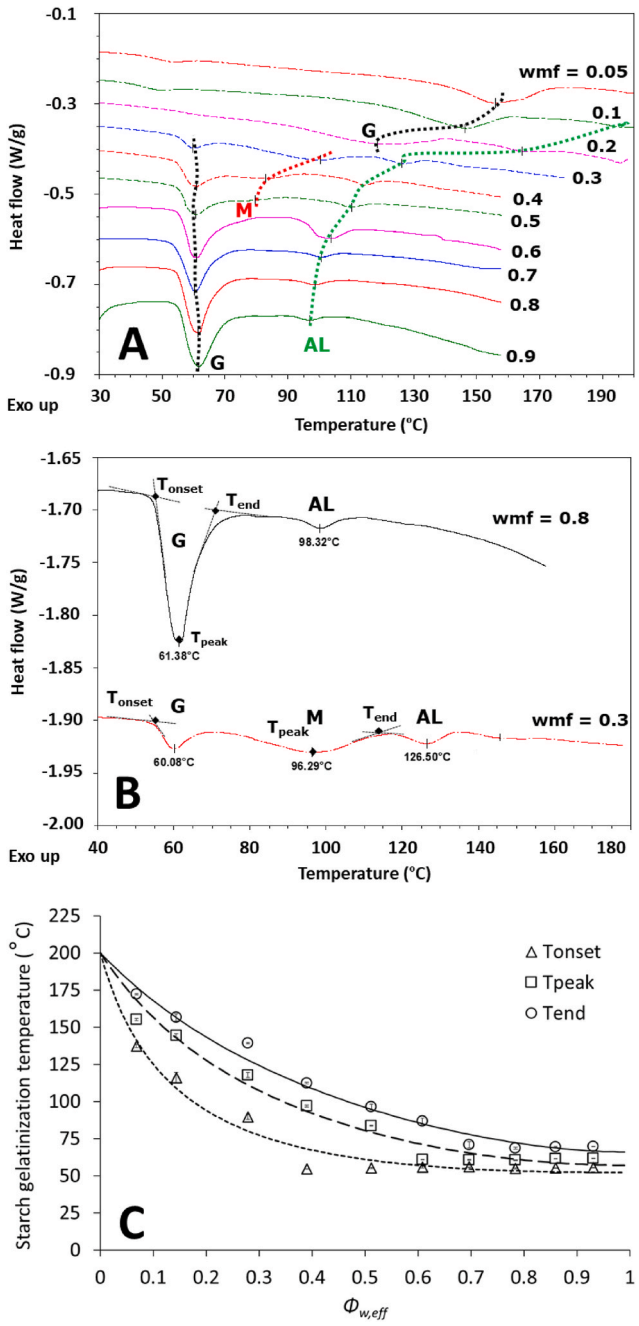

Fig. 1. [A] Starch gelatinization profile from DSC thermograms for various hydration levels expressed as water mass fractions (wmf). The dotted lines indicate the different endotherms observed: G = gelatinization accompanied by the uptake of water (Donovan, 1979) (dotted black line); M = melting of crystals (Donovan, 1979; Evans & Haisman, 1982) (dotted red line); AL = melting of amylose-lipid complexes (dotted green line). [B] At high water contents (i.e. 0.8 wmf), one main peak is observed around 60 °C (Steeneken & Woortman, 2009). At intermediate water contents (i.e. 0.5–0.3 wmf), a broadening of the starch gelatinization peak is observed with the occurrence of three peaks. Based on the description of the different stages of re-organization during starch melting (Waigh et al., 2000), G is defined as smectic/isotropic re-ordering of double helices; M as the main melting event resulting in loss of crystallinity following on the unwinding of double helices via helix/coil transitions [C] Starch gelatinization profile (i.e. T_{onset}, T_{peak} and T_{end}); as described by $\Phi_{w,eff}$ at different levels of hydration (0.9–0.05 wmf, symbols) following on the application of FH theory for biopolymer melting (model predictions are indicated by solid and dotted lines). Error bars representing standard deviation are included for each symbol. (For interpretation of the references to colour in this figure legend, the reader is referred to the Web version of this article.)

endotherm.

The gelatinization behaviour, i.e. T_{onset}, T_{peak} and T_{end}, of wheat starch as derived from the analysis of DSC thermograms was plotted as a function of $\Phi_{w,eff}$ (which for the water solution is then equal to Φ_{water}; equation (4)), as shown in Fig. 1C. T_{onset}, T_{peak} and T_{end} data were modelled using the FH theory (equation (5)). The fitted parameters were $T_{m,0}$, ΔH_U, and the degree of crystallinity ξ (Van Der Sman & Meinders, 2011). Via regression we obtained $T_{m,0}$ = 473 (K), $\Delta H_{U,T_{onset}}$ = 25.1 kJ/mol, $\Delta H_{U,T_{peak}}$ = 26.4 kJ/mol, $\Delta H_{U,T_{end}}$ = 28.9 kJ/mol, ξ_{onset} = 0.66, ξ_{peak} = 0.25 and ξ_{end} = 0.

4.2. Starch gelatinization in solutions of sugars and sugar replacers

Similar to our recent study on egg white proteins denaturation (Renzetti et al., 2020), we here tested the hypothesis that starch gelatinization in presence of sugars and sugar replacers can be quantitatively described by $\Phi_{w,eff}$, following on its application in the FH theory for biopolymer melting (van der Sman, 2016). For such purpose, plasticizers belonging to different classes of compounds were used including sugars, polyols, amino acids and soluble fibres comprising various oligofructoses and a polydextrose. A broad range of starch to solvent ratio's were tested similar to the experiments in water solutions. The $\Phi_{w,eff}$ of the different solutions in this study was computed by using the dry $T_{g,s}$ and other material properties listed in Table 3, according to equations (1) and (5).

According to our hypothesis, the different sugar and sugar replacers solutions as well as the variations in starch:solvent ratio's tested would alter the $\Phi_{w,eff}$ of the solvent, resulting in a shift in T_{onset}, T_{peak} and T_{end} of gelatinization. This effect is clearly shown in Fig. 2 and Fig. 3 for various concentrations (i.e. 15, 30 and 50% w/w) of glucose, sucrose and OFP at two different starch:solvent ratio's. At starch:solvent ratio of 1:4, the hydration level is such that only the endotherm G can be observed for the gelatinization process (Fig. 2). For each sugar solution, increasing sugar concentration results in a decrease in $\Phi_{w,eff}$ and consequently in an increase in gelatinization temperature (i.e. T_{peak}). At similar concentrations, differences in sugar type affects $\Phi_{w,eff}$ due to differences in their $N_{OH,s}$ and in their molar volumes. Consequently shifts in T_{peak} are observed. At higher starch concentrations as in Fig. 3 (i.e. starch:solvent ratio of 3:2), the DSC thermograms in water, glucose, sucrose and OFP solutions show the decoupling of the G and M stages of gelatinization. Overall, the DSC thermograms of starch in presence of sugars show similar melting transition as those obtained in pure water for different levels of hydration. However, changes in $\Phi_{w,eff}$ as affected by sugar type and concentration promoted the shift in both G and M transitions towards higher temperatures compared to pure water.

Table 3
Chemical-physical characteristics of the investigated compounds.

Compound	M_w (g/mol)	Density (kg/m^3)	T_g (K)	$N_{OH,s}$	$N_{OH,s}/v_s$ (1000 mol/cm^3)
Water	18	1000	139	2	111.1
Glycine	75	1660	220[a]	2.63	58.2
Proline	115	1370	250[a]	2.99	35.6
Xylitol	152	1520	249	2.94	29.4
Glucose	180	1540	306	4	34.2
Sucrose	342	1550	336	4.48	20.3
FOS Actilight (FOS)	605	1550	315[b]	4.66	11.9
Frutalose OFP (OFP)	725	1550	328[b]	5.16	11.0
Frutafit CLR (CLR)	1769	1550	362[b]	7.24	6.3
Polydextrose Litesse Ultra (PDX)	2160	1550	366[b]	6.16	4.4
Frutafit IQ (IQ)	2184	1550	372[c]	8.09	5.7
Frutafit TEX (TEX)	3877	1550	421[c]	23.18	9.3

[a] From (van der Sman & Mauer, 2019).
[b] From Renzetti et al., 2020.
[c] Computed from Flory-Fox equation.

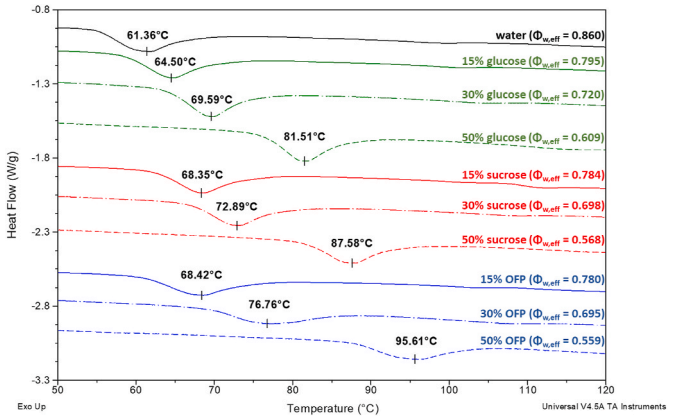

Fig. 2. DSC thermograms of starch gelatinization profile (i.e. T_{peak} is indicated for each thermogram) in water, glucose, sucrose and OFP solutions performed at a constant starch:solvent ratio of 1:4. The high solvent to starch ratio results in one main gelatinization endotherm, independently of the sugar concentration. For each solution in the thermograms, the computed $\Phi_{w,eff}$ is indicated, showing the effect on shifting T_{peak} as function of sugar concentration and sugar type.

The T_{peak} of starch gelatinization in 15, 30 and 50% solutions of glucose, sucrose, OFP and proline in water is shown in Fig. 4 for all the starch:solvent ratio's tested in this study. For all these solutions, the T_{peak} of starch gelatinization follows the FH master curve obtained for starch:water mixtures, based on changes in $\Phi_{w,eff}$. Similar results were observed for T_{onset} and T_{end}, which could be also well described by the FH model for glucose, sucrose, OFP (Fig. 5) and proline (data not shown). By looking at Figs. 4 and 5 it can be clearly observed that at sugar concentrations of 50%, the FH model seem to best describe the T_{end} gelatinization while largest deviations were observed for T_{onset}. For T_{peak} deviations were observed only for $\Phi_{w,eff}$ >0.5, hence in conditions where helix-helix side chains dissociation and the helix-coil transition merge into a single G endotherm. Furthermore, deviations from the FH model at 50% plasticizer concentrations seem to follow the order OFP > sucrose > glucose. On the contrary, no deviations in FH model predictions of T_{onset} were observed for solutions with proline (data not shown). Differences in the ability of the FH model to predict T_{onset} and T_{end} have been previously reported (van der Sman, 2016), but were not yet related to specific dependencies on plasticizer type and concentration.

The FH model predictions were also tested for a 30% xylitol solution, the soluble fibres listed in Table 1 and the ternary and quaternary mixtures of Table 2. As shown in Fig. 6, the T_{peak} of starch gelatinization could be well described by the FH model for all those solutions. Only for a 30% solution of TEX at a solvent mass fractions of 0.5 a large deviation from the FH model was observed.

In a recent study on egg white denaturation in sugar and sugar replacer solutions (Renzetti et al., 2020), deviations from the FH model predictions were observed for $\Phi_{w,eff}$>0.3. For similar $\Phi_{w,eff}$values, the deviations were assumed to be due to phase separation driven by plasticizer concentration and by the number of effective hydroxyl groups per molar volume of the plasticizers (or plasticizers mixture) $N_{OH,s}/v_s$.

The larger the $N_{OH,s}/v_s$ of the plasticizer the larger the phase separation, resulting in an elevation of the denaturation temperature due to a reduction in the effective hydrogen bond density in the protein-rich domain. In order to check whether the same mechanism applied to the starch gelatinization conditions of this study, the T_{peak} of starch gelatinization experimentally obtained in conditions of $\Phi_{w,eff}$ equal to 0.6 (±0.02), i.e. excess solvent condition, were plotted as function of the $N_{OH,s}/v_s$ of the plasticizer or plasticizers mixture (Fig. 7). Contrary to what observed for egg white (Renzetti et al., 2020), T_{peak} increased with a reduction in $N_{OH,s}/v_s$ which would not associate with a phase

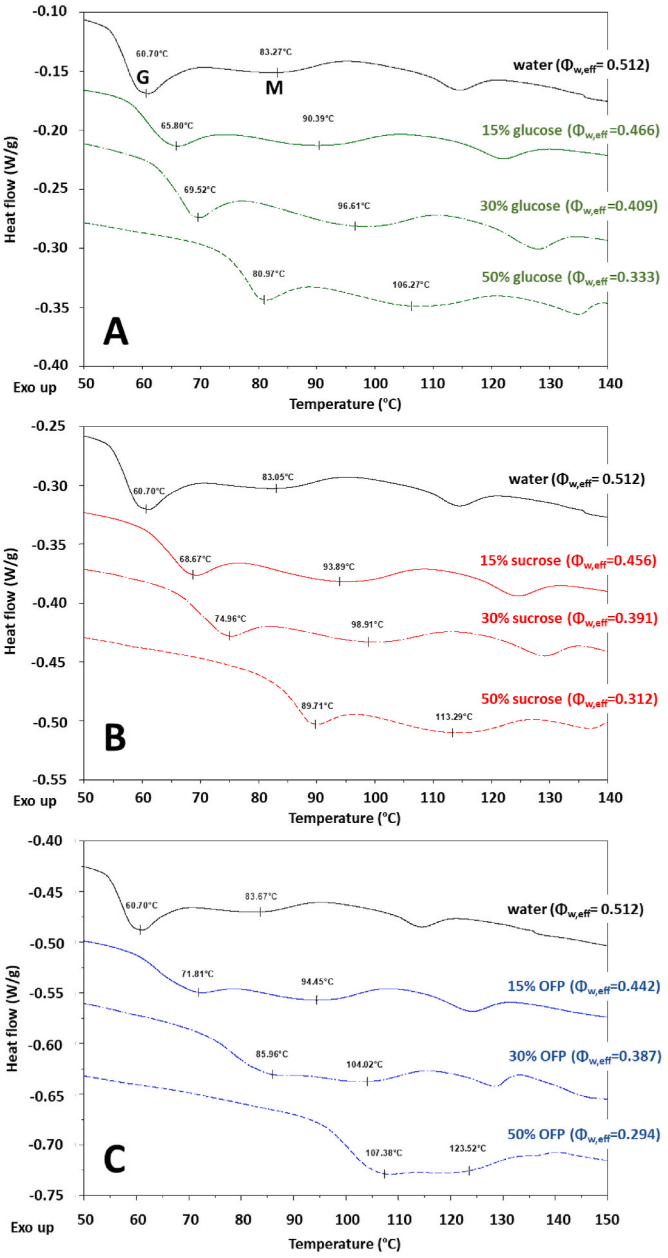

Fig. 3. DSC thermograms of starch gelatinization profile (i.e. T_{peak} is indicated for each thermogram) obtained at a constant starch:solvent ratio of 3:2. Different concentrations of [A] glucose, [B] sucrose and [C] OFP are shown as compared to the starch:water solution at similar ratio. The low hydration conditions results in the two stage process of gelatinization (Waigh et al., 2000), showing the G and M endotherms. For each solution in the thermograms, the computed $\Phi_{w,eff}$ is indicated, showing the effect on shifting both G and M (i.e. T_{peak}) as function of sugar concentration and sugar type.

separation effect induced by small solutes. Furthermore, the change in T_{peak} seemed to follow a sigmoidal function, with a minimum T_{peak} for low M_w plasticizers ($N_{OH,s}/v_s$ > 29) and a maximum in T_{peak} for high M_w plasticizers ($N_{OH,s}/v_s$ < 10) (Fig. 7).

4.3. Starch pasting behaviour in solutions of sugars and sugar replacers

Starch pasting behaviour was studied in an RVA for different sugar and sugar replacers concentrations (i.e. 10, 20, 30 and 40%) while keeping a fixed starch amount (8% dm). The pasting profiles of wheat starch in various sugar and sugar replacers solutions of 20 and 40%

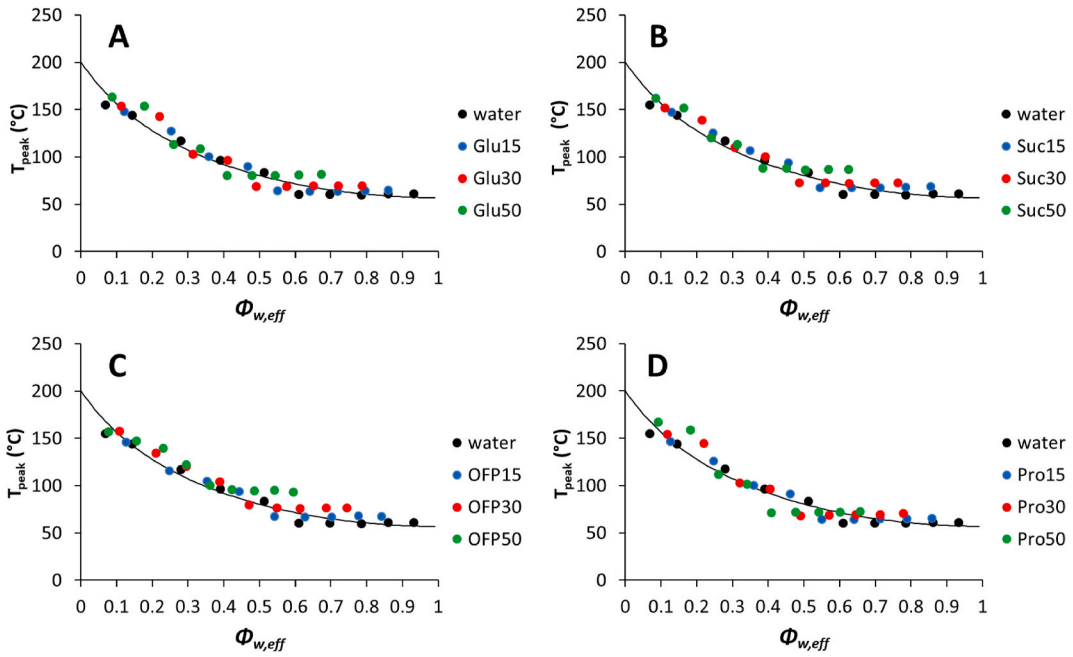

Fig. 4. T_{peak} of starch gelatinization as described by $\Phi_{w,eff}$, for 15, 30 and 50% solutions in water of glucose [A], sucrose [B], the oligo-fructose Frutalose OFP [C] and proline [D]. All tests were performed using starch concentrations ranging mass fraction from 0.05 to 0.9.

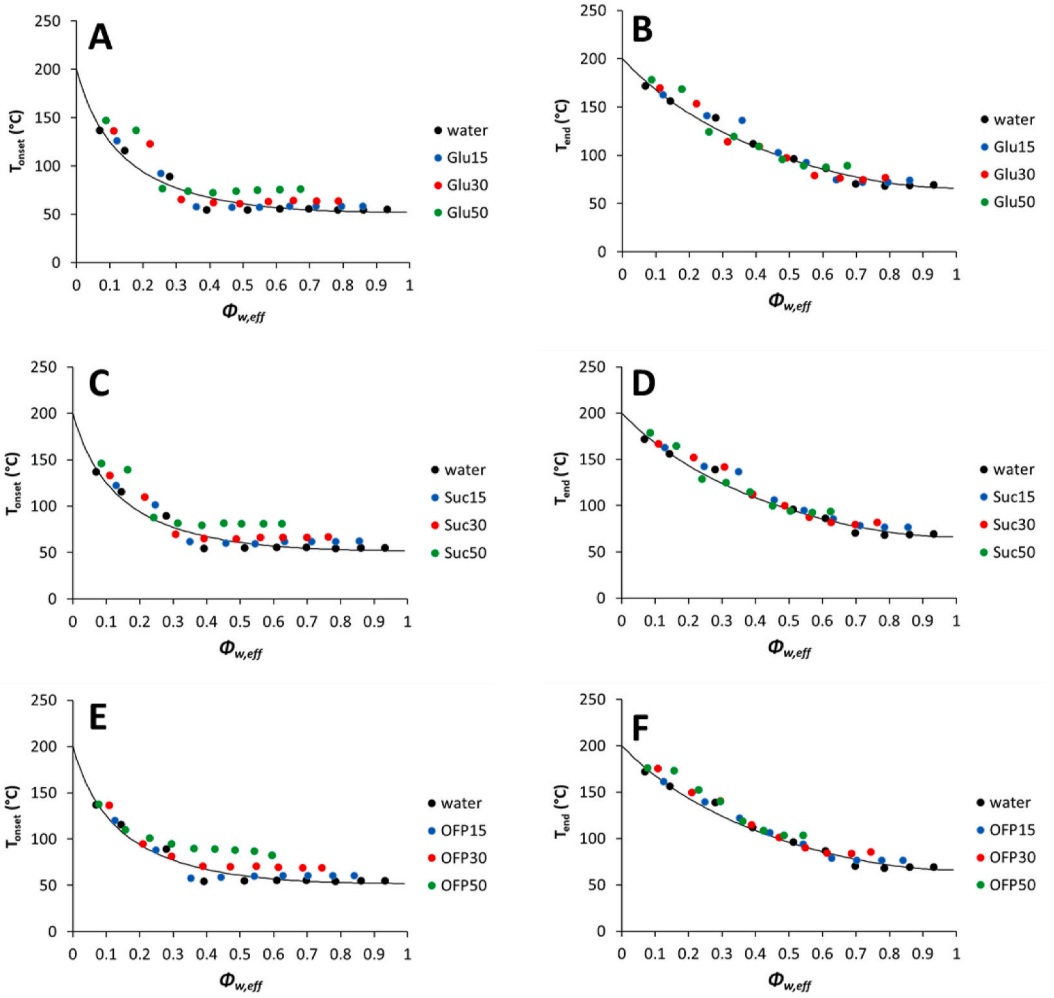

Fig. 5. T_{onset} and T_{end} of starch gelatinization as described by $\Phi_{w,eff}$ for 15, 30 and 50% solutions in water of glucose [A,B], sucrose [C,D] and the oligo-fructose Frutalose OFP [E, F]. All tests were performed using starch concentrations ranging in mass fraction from 0.05 to 0.9.

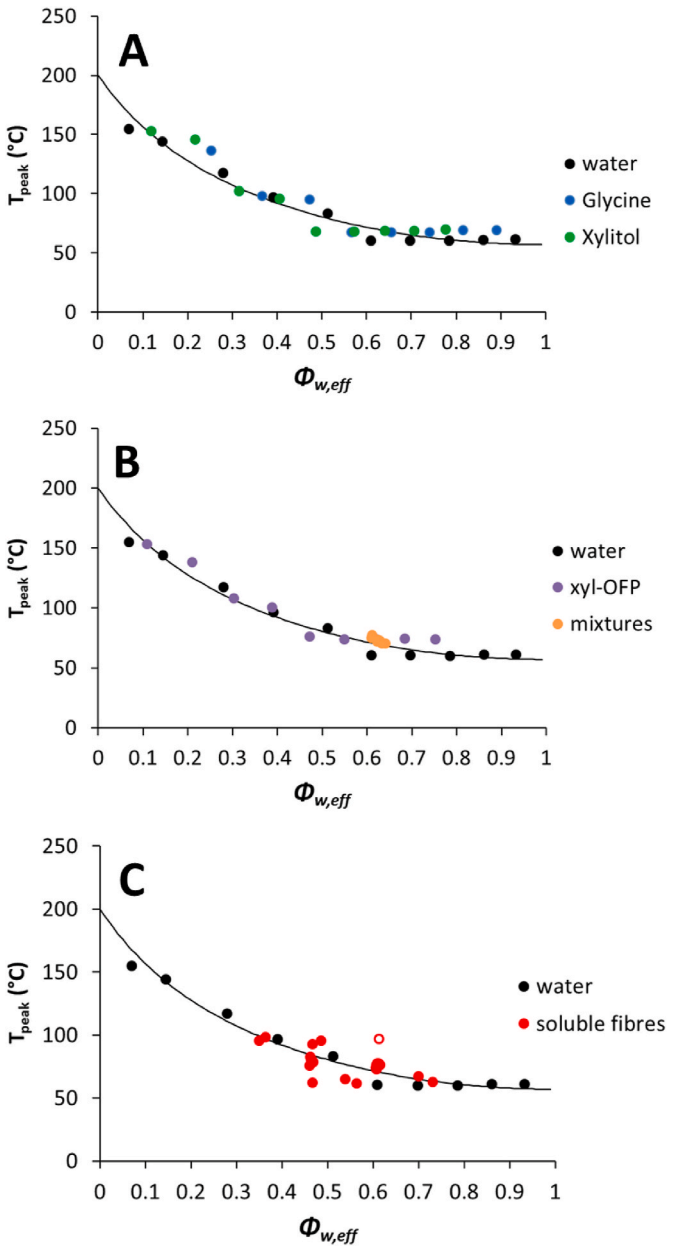

Fig. 6. T_{peak} of starch gelatinization as described by $\Phi_{w,eff}$, for 30 solutions in water of glycine and xylitol [A]; a binary mixture of xylitol and OFP as well as mixtures from Table 2 [B]; soluble fibres from Table 1 [C]. All tests were performed using starch concentrations ranging mass fraction from 0.05 to 0.9, except for mixtures and soluble fibres in B and C, respectively, which were tested at solvent mass fractions of 0.7 and 0.5. In figure C, the red open circle represents the 30% Frutafit TEX solution at solvent mass fraction of 0.5. (For interpretation of the references to colour in this figure legend, the reader is referred to the Web version of this article.)

concentration (w/w) are shown in Fig. 8A and B, respectively. At 20% concentration, all sugar and sugar replacers solutions showed a general increase in paste viscosity (i.e. peak viscosity and final viscosity) as compared to water only. The peak viscosity represents the maximum swelling of intact starch granules during gelatinization, before rupture of granules occurs with solubilization and further leaching out of amylose. In general, the increase in peak viscosity was largest for the low M_w plasticizers compared to the higher M_w like FOS or FOS containing mixtures. The influence of the M_w of the plasticizers became further evident at 40% concentration. For low M_w sugars (up to 342 g/mol), increasing concentration from 20 to 40% further enhanced paste viscosity compared to pure water (Fig. 8A and B). On the contrary, for high M_w sugar replacers like FOS or FOS containing mixtures, a reduction in peak and final viscosity was observed compared to 20% concentration. The effect of high M_w plasticizers in suppressing swelling and paste viscosity of starch was even more evident when different soluble fibres were tested at 30% concentration (see Fig. 8C). In general, the higher the M_w the larger the reduction in paste viscosity (e.g. peak viscosity). With the inulin IQ and TEX, almost no viscosity build up could be observed during the RVA experiment. Interestingly, all the DSC traces of starch suspension in 30% fibre solutions in excess solvent (as in the pasting experiment of Fig. 8C) showed starch gelatinization endotherms (Fig. 8D). Hence, gelatinization occurred without building up in paste viscosity (i.e. swelling and amylose leaching). For soluble fibres with M_w as high as 1769 g/mol, i.e. CLR, the T_{peak} of gelatinization seemed to follow the trend of an increase in gelatinization temperature with reduction in $\Phi_{w,eff}$ (see Fig. 8D). For fibres with $M_w > 1769$ g/mol as IQ and TEX, the DSC traces showed a distinct profile with two melting peaks appearing in the 60-100 °C range, as if the gelatinization process was occurring differently than with the smaller soluble fibres. From the analysis of the pasting curves it was evident that the interplay of plasticizer type and concentration affected the pasting behaviour of starch.

In order to further analyze such behaviour, the peak viscosities obtained for all sugar and sugar replacers solutions were plotted as function of plasticizer concentration, as shown in Fig. 8E. Compared to the suspension of starch in pure water, additions of sugars and sugar replacers generally showed an increase in peak viscosity. However, the dependency on concentration seemed to be specific for the plasticizer type. While glucose, xylitol and proline showed an almost linear increase in peak viscosity till 40%, sucrose and maltitol seemed to level off at 40%. Furthermore, all FOS containing solutions showed a maximum in peak viscosity at 20% while further increases resulted in a progressive reduction. Similar results were also found for the final viscosity (data not shown). Additionally, starch pasting temperatures in all sugar and sugar replacer solutions showed a decrease till 20% concentration, followed by an increase with higher sugar and sugar replacer concentrations (Fig. 8F). In general the pasting temperature was lower than in pure water, with few exceptions.

Peak viscosities were plotted as function of $\Phi_{w,eff}$ for all starch suspensions studied in the RVA in order to check whether this parameter could universally explain the observed effects of plasticizer type and concentration (Fig. 9A). However, no universal trend was observed, thus indicating that the effective volume fraction of hydrogen bonds in solution cannot explain alone the mechanisms of solvent ingress and starch swelling during pasting. The influence of an intrinsic property of the plasticizers, i.e. $N_{OH,s}/v_s$, on starch pasting was then tested by plotting all the peak viscosities obtained at 30% concentration of sugar and sugar replacers as function of $N_{OH,s}/v_s$ (Fig. 9B). These variations included single plasticizers solution in Table 1 and the binary and ternary mixtures in Table 2. The $N_{OH,s}/v_s$ of mixtures was computed according to equation (4). A sigmoidal distribution of viscosities was observed with peak viscosity leveling off to a maximum for $N_{OH,s}/v_s > 20$ (1000 mol/cm^3). Below 20, the peak viscosity sharply decreased and became significantly lower than the one in pure water for $N_{OH,s}/v_s \leq 10$ (1000 mol/cm^3) ($p < 0.05$). Hence, depending on plasticizer type (i.e. $N_{OH,s}/v_s$) starch swelling could be either enhanced or inhibited as compared to pure water solutions. An adapted Fermi distribution function was developed to describe these results:

$$Peak\ viscosity\ (cP) = \frac{PV_{max} - PV_{min}}{1 + e^{\left(\frac{-\frac{N_{OH,s}}{v_s} + \left(\frac{N_{OH}}{v}\right)_{critical}}{b}\right)}} + PV_{min} \quad (8)$$

where PV_{max} and PV_{min} are the maximum and minimum viscosity, respectively, $\left(\frac{N_{OH}}{v}\right)_{critical}$ is the critical value at which the peak viscosity

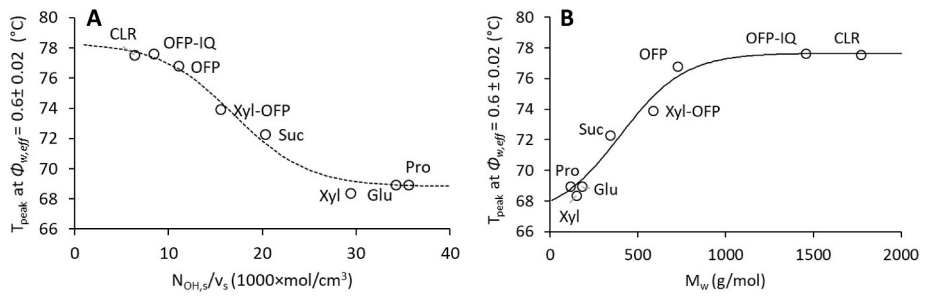

Fig. 7. T_{peak} of starch gelatinization measured at conditions of $\Phi_{w,eff} = 0.6$ (±0.02) for 30% sugars and sugar replacers solutions in water and plotted as function of $N_{OH,s}/v_s$ and M_w of the plasticizers. In case of mixtures, the average values were computed. Pro = proline, Glu = glucose, Xyl = xylitol, Suc = sucrose, OFP=Frutalose OFP, IQ=Frutafit IQ, CLR=Frutafit CLR.

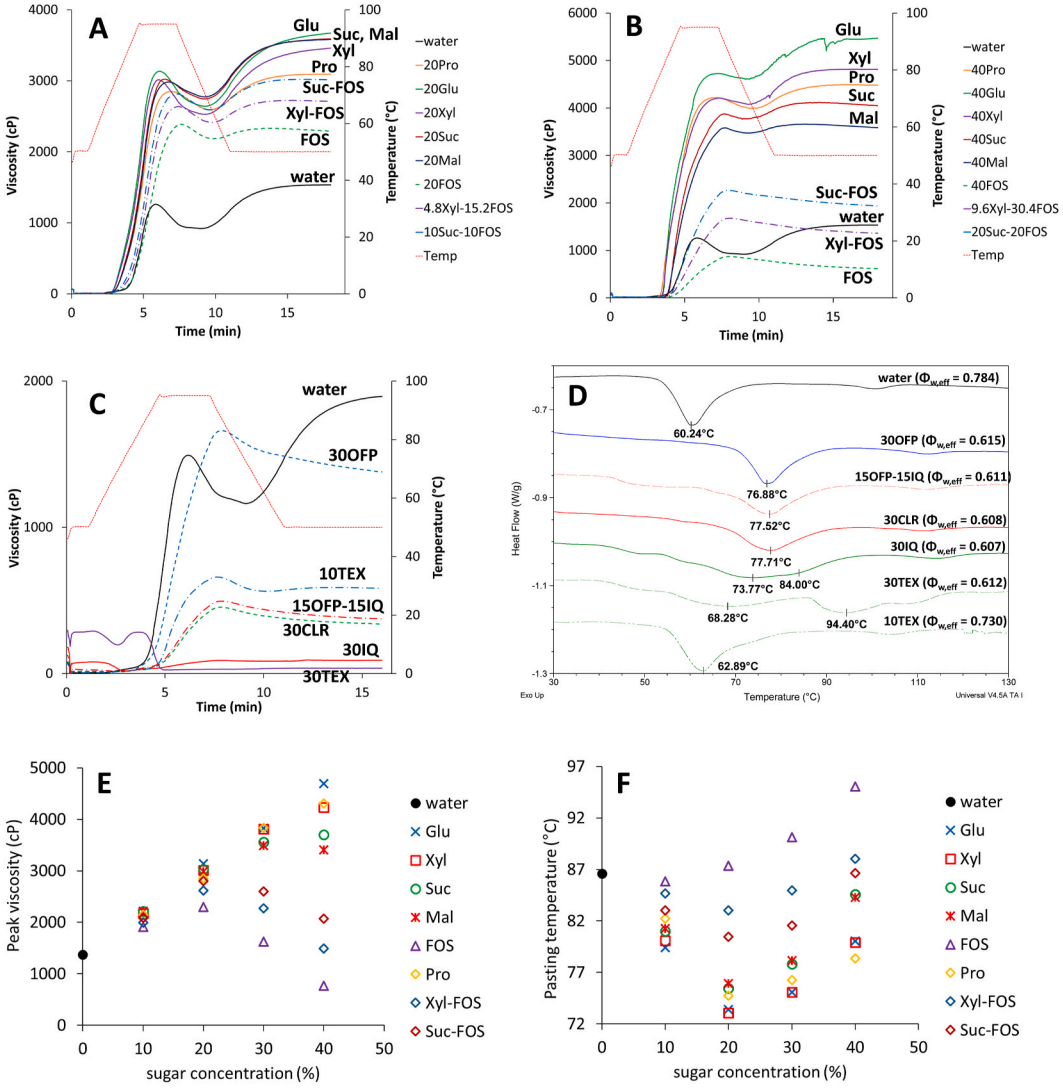

Fig. 8. RVA profile of 8% (dm) wheat starch in water and sugar solution of 20% [A] and 40% [B] and in 30% soluble fibres solutions as well as TEX at 10% solution [C]. DSC thermograms of starch (0.3 starch mass fraction) in soluble fibres solutions [D]. Peak viscosities [E] and pasting temperatures [F] obtained as function of sugar concentrations and sugar types. Pro = proline, Glu = glucose, Xyl = xylitol, Suc = sucrose, Mal = maltitol, OFP=Frutalose OFP, FOS=FOS Actilight, IQ=Frutafit IQ, CLR=Frutafit CLR, TEX = Frutafit TEX. Details on composition of mixtures is provided in Table 2.

is equal to $\frac{PV_{max} - PV_{min}}{2}$ and b is constant accounting for the steepness of the relationships around $\left(\frac{N_{OH}}{v}\right)_{critical}$. The model was tested for all sugar concentrations of this study using a non-linear least squares regression.

As shown in Fig. 9B and C, all peak viscosity data for each sugar concentration followed the adapted Fermi model ($R^2 > 0.98$, $p < 0.05$ for all data sets). The obtained values of the Fermi model parameter are reported in Table S1. Increasing sugar concentration resulted in a

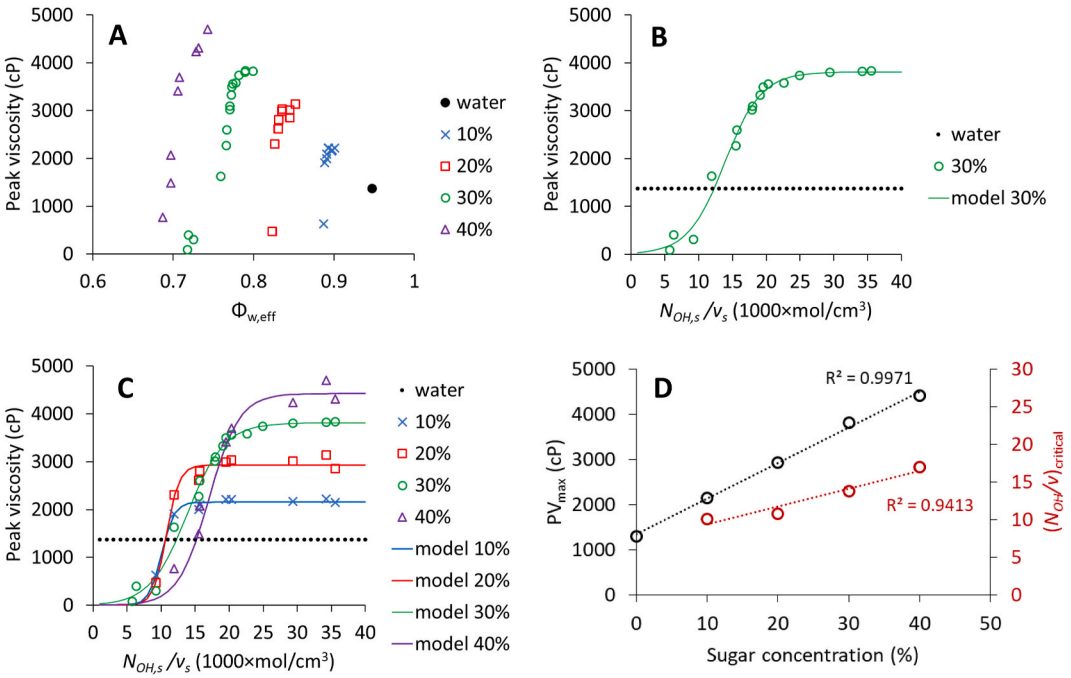

Fig. 9. Peak viscosities plotted as function of $\Phi_{w,eff}$ [A] and as function of $N_{OH,s}/v_s$ in 30% sugar solutions [B] as well as in 10, 20 and 40% sugar solutions [C]. The continuous lines in [B, C] represent the predictions from the adapted Fermi model described in the text. The dotted lines in [B, C] represent peak viscosity as obtained in pure water. The fitting parameters PV_{max} and $\left(\frac{N_{OH}}{v}\right)_{critical}$ from the Fermi model of equation (8) are plotted as function of sugar concentration [D].

progressive increase of PV_{max} in the Fermi model of equation (8) (Fig. 9D), while PV_{min} was always zero. Furthermore, the characteristic $\left(\frac{N_{OH}}{v}\right)_{critical}$ also increased linearly with increasing plasticizer concentration.

Both the onset temperatures for pasting and gelatinization temperatures at excess solvent (only G endotherm present in DSC traces) showed similar trends in relation to $N_{OH,s}/v_s$ (Fig. S1). Contrary to what observed for the pasting temperatures (Fig. 8F), the gelatinization temperatures were far higher than in pure water.

5. Discussion

The working hypothesis of this study was that the starch gelatinization process is driven by hydrogen bonding interactions between the starch and the solvent (i.e. the water-sugar mixtures) and that the solvent properties can be quantitatively described by the volumetric density of hydrogen bonding sites available in the solution, i.e. $\Phi_{w,eff}$. As the starch-solvent system is heated, the solvent would penetrate into the granules and disrupt the hydrogen bonds that govern the amylopectin helix–helix associations and double helices. From such perspective, the hydrogen bonding ability of the solvent treated as a whole would govern the gelatinization process. Several sugars and sugar replacers solutions were used in this study, comprising different classes of compounds, i.e. mono and disaccharides, sugar alcohols, amino acids, soluble fibres and mixtures thereof. The approach allowed to evaluate how intrinsic properties of the sugars and sugar replacers, i.e. $N_{OH,s}/v_s$, would contribute to the plasticizing properties of the solvent, including solvent ingress and granule swelling. Following a sidechain liquid crystalline model proposed by (Waigh et al., 2000), the analysis of the DSC traces of starch suspensions in pure water allowed us to depict the gelatinization behaviour (i.e. T_{onset}, T_{peak} and T_{end}) over the entire range of $\Phi_{w,eff}$. The T_{onset}, T_{peak} and T_{end} could be well described by applying the FH theory for biopolymer melting (Fig. 1C).

The starch gelatinization observed in the DSC traces with the presence of sugars and sugar replacers (with M_w till 2000 g/mol) were similar to those of the starch-water mixtures at both excess (Fig. 2), intermediate (Fig. 3) and limited (data not shown) solvent levels. Only a temperature shift in the endotherms was observed, which related to the specific effect of the sugar and sugar replacers types and concentrations on the $\Phi_{w,eff}$. In fact, the FH model extended with $\Phi_{w,eff}$ predicts a shift in gelatinization temperature of wheat starch in presence of sugars and sugar replacers, and not a change in the molecular mechanisms (Figs. 2 and 3). These results are consistent with earlier hypothesis that gelatinization is controlled by the plasticizing ability of the solvent (Donald, 2001). With pure water being the most effective H-bonding solvent (as indicated by its high $N_{OH,s}/v_s$ in Table 3), the addition of non-aqueous solutes (such as sugar and sugar replacers) to pure water would reduce the level of solvent plasticization. From such standpoint, the solvent effectiveness would highly depend on properties such as molecular size, viscosity, diffusivity and hydrogen bonding capacity (Tan et al., 2004; Perry & Donald, 2002; Perry & Donald, 2000).

Overall, the proposed FH model could well describe the T_{onset}, T_{peak} and T_{end} of wheat starch gelatinization in presence of different sugars and sugar replacers at various concentrations and levels of solvation (Figs. 4-5). For the various sugar solutions in this study, $\Phi_{w,eff}$ was derived from $N_{OH,s}/v_s$ of each plasticizing molecule following from equation (5). The effective number of hydrogen bonding sites per molecule, i.e. $N_{OH,s}$, accounts for differences in stereochemistry among sugars and sugar replacers, as the distribution of hydroxyl groups between exocyclic, equatorial and axial affects the hydrogen bonding ability of the plasticizer (Uedaira, H. & Uedaira H., 1985) (Miljkovic, 2010) (Allan et al., 2018). Hence, $N_{OH,s}/v_s$ provides the volume density of effective hydrogen bonds for each plasticizer, thus accounting for both the specific hydrogen bonding ability and the molecular size factors suggested by Tan et al. (2004) and Perry and Donald (2002). It also quantifies the plasticizers contribution to the solvent properties in terms of both quantity and quality, i.e. $\Phi_{w,eff}$, which govern starch gelatinization.

Large deviations from the FH model predictions were observed at 50% sugar concentration for T_{onset} with $\Phi_{w,eff}$ >0.3 (Fig. 5A,C,E) and only slight deviations for T_{peak} with $\Phi_{w,eff}$ >0.5 (Fig. 4). Instead, no

deviations were observed for T_{end} (Fig. 5B,D,F). It is well documented that phase separation phenomena occur in biopolymer-sugar-water systems at intermediate sugar concentrations (i.e. 37-60%) resulting in a biopolymer-rich and a sugar-rich phase with water partitioned over the two phases (Roudaut & Wallecan, 2015; Ubbink, 2016; van der Sman, 2019; (Renzetti et al., 2020; Lerbret et al., 2007; Lins, Pereira, & Hünenberger, 2004; Kawai & Hagura, 2012). In such conditions, the $\Phi_{w,eff}$ does not represent the H-bonding environment around the biopolymer as the sugars will contribute less to the intermolecular hydrogen bonds with the biopolymer. Phase separation is mainly driven by the molecular size (Ubbink, 2016; van der Sman, 2019) and by the $N_{OH,s}/v_s$ of the plasticizer or plasticizers mexture (Renzetti et al., 2020), with small molecules being more effective in inducing phase separation than larger ones. In this study, starch gelatinization temperature at a constant $\Phi_{w,eff}$ value of about 0.6 increased with a reduction in $N_{OH,s}/\ v_s$ (Fig. 7A), hence with an increase in M_w, following a sigmoidal function till a steady value for $M_w > 1000$ g/mol (Fig. 7B). This is contrary to what previously observed for egg white proteins in sugar solutions (Renzetti et al., 2020). Phase separation undoubtedly occurs at 50% sugar concentration, as indicated by the deviations of T_{onset} from the FH model for all sugars and sugar replacers (Fig. 5). However, it can be suggested that an additional mechanism is affecting the gelatinization process, other than the plasticizing (i.e. H-bonding ability) properties of the solvent and phase separation at high sugar concentrations. It should be noted that the solvent properties described by $\Phi_{w,eff}$ as applied in the FH model consider gelatinization as a phase transition from a crystalline to an amorphous-rubbery state, assuming a thermodynamic equilibrium between the crystalline state and the rubbery state. Considering the semi-crystalline nature of starch, with interconnected amorphous and crystalline regions, the gelatinization process is most likely controlled by the interplay of both non-equilibrium (kinetic) factors, related to solvent penetration and starch swelling, and equilibrium (thermodynamic) factors related to the melting process.

The amorphous phase plays a significant role in the phase transition of granules during gelatinization, as a certain degree of swelling in the amorphous lamellae region must occur to transmit disruptive stress to the crystalline regions through connecting molecules (Jenkins & Donald, 1998). Several studies suggest that the G endotherm in the DSC profiles represents the energy change mainly associated with solvent absorption and granule swelling to its maximum (Jenkins & Donald, 1998; Wang et al., 2014; Wang et al., 2016; Kovrlija & Rondeau-Mouro, 2017). A significant reduction in the crystallinity levels of starch granules occurs only at temperatures higher than the peak temperature of the G endotherm (Jenkins & Donald, 1998; Bail et al., 1999; Svensson & Eliasson, 1995). In this context, the side-chain liquid-crystalline model of (Waigh et al., 2000) provides an explicit molecular mechanism for the 'swelling driven processes', where the side-by-side helix dissociation is viewed as an indicator of solvent ingress, which subsequently produces swelling of the crystalline growth rings (Tananuwong & Reid, 2004). Hence, it is reasonable to suggest that the swelling process, which includes the helix-helix dissociation, and the melting of the crystalline domains can be viewed as two distinct processes. The first would be affected by an interplay of kinetic and thermodynamic factors and the second by thermodynamics. As a result, the observed deviations from the FH model at 50% sugar concentrations for T_{onset} and for T_{peak} (in excess solvent where only the G endotherm appears) may be well related to the influence of kinetic aspects. In fact, the hydration and swelling (plasticization) mechanisms in sugar solutions are the same as in water (Perry & Donald, 2000; Donald, 2001). Only the temperature/time at which these processes take place are dependent on the plasticization ability of the solvent and the ability to penetrate the granules, which are related to viscosity and molecular sizes (Perry & Donald, 2000). Water enters the granule more easily than any other solvent, while providing the highest molar density of H-bonding sites, i.e. $N_{OH,s}/v_s$. Thus water provides a baseline against which other solvents can be compared. We here suggest that the solvent properties involved in the plasticization and swelling process can be mainly related to the intrinsic properties of the plasticizers, $N_{OH,s}/v_s$, and the resulting effects on the overall hydrogen bonding ability of the solvent, i.e. $\Phi_{w,eff}$. The swelling behaviour as observed in the RVA experiments is discussed in the next paragraphs to support this hypothesis.

For a fixed sugar and sugar replacers concentration, the swelling behaviour (i.e. peak viscosity) of starch was controlled by the $N_{OH,s}/v_s$ of the plasticizer, as described by the adapted Fermi model of equation (8). The model predicted a maximum swelling at high values of $N_{OH,s}/v_s$(low M_w) as well as inhibition of swelling at low values of $N_{OH,s}/v_s$(high M_w) as compared to pure water. With increasing plasticizer concentration, the maximum peak viscosity PV_{max} from the Fermi model increased with a concomitant increase in $\left(\frac{N_{OH}}{v}\right)_{critical}$ (Fig. 9D). There are several factors which may contribute to the observed pasting behaviour as function of $N_{OH,s}/v_s$ and plasticizer concentration. These factors can be mainly associated to solute partitioning, solvent viscosity and molecular size affecting the kinetics and extent of solvent ingress into the granules. Additionally, soluble polymers with high M_w can influence the effective concentration of starch as a result of water retained by the fibre (Tester & Sommerville, 2003; Khanna & Tester, 2006), thus inhibiting starch swelling and amylose leaching (Hou et al., 2020).

As recently observed for swelling of polysaccharides microgels, sugars do not compete with starch for water, but acts more synergistically in maintaining hydrogen bonding with the solvent (van Der Sman, 2018). Therefore, more solvent needs to enter the starch granule to achieve the same level of plasticization compared to pure water. Sugars will partition between the polymer phase and the solution phase, with the partitioning coefficient increasing with increasing sugar concentration and with decreasing M_w of the sugar (van Der Sman, 2018), resulting in increased swelling. Partitioning is governed by the starch-solvent interaction parameter χ from Flory-Rehner theory, which has been recently shown to be function of solvent properties, i.e. $\Phi_{w,eff}$ (van Der Sman, 2018). Consequently, small molecule with high values of $N_{OH,s}/v_s$ contribute to a higher starch-solvent interaction than large ones. In agreement with these mechanisms, the results of this study showed enhanced peak viscosity with increasing sugar concentration and with decreasing M_w, i.e. increasing $N_{OH,s}/v_s$, (Fig. 9C).

Swelling can be regarded as a two-step process with a long tailing towards steady-state after the initial exponential increase (van Der Sman, 2018). Hence, experimental results in the conditions of the RVA tests show non-equilibrium conditions. Increasing viscosity contributes to slowing down the second step towards equilibrium (van Der Sman, 2018). As the viscosity of sugar and sugar replacer solutions is inversely related to the effective hydrogen bond density of the solution (van der Sman & Mauer, 2019; Renzetti et al., 2020), a decrease in $N_{OH,s}/v_s$ associated with increasing M_w will further slowdown the swelling kinetics. This mechanism is in agreement with the observation that with increasing plasticizer concentration up to 40%, only small plasticizers, i.e. those with $N_{OH,s}/v_s > 25$ (1000 mol/cm^3) like glucose, proline and xylitol (Table 3), showed enhanced swelling compared to the 30% solutions. Indeed, water mobility in sugar/water/starch system is affected by the M_w of the plasticizer (Lim, Setser, & Paukstelis, 1992) and the T_{peak} of the G endotherm also correlates with the viscosity of the solution around that temperature (van der Sman & Mauer, 2019). Hence, solvent viscosity likely contributes to the gelatinization process in relation to the plasticization and swelling of the starch granules. Our results confirm the importance of viscosity effects at similar $\Phi_{w,eff}$ (Fig. 7) in excess solvent conditions. At $\Phi_{w,eff}$ equal to about 0.6 (hence where only the G endotherm appears), increasing M_w up to ~800 g/mol increased the T_{peak} beyond what predicted from the FH model.

The ability of molecules to enter starch granules is determine by their size, with plasticizers having a M_W greater than ~1000 being unable to enter the starch granules (French, 1984). Kim and Setser (1992)

reported that soluble fibres, i.e. fractionated polydextrose and maltooligosaccharides, of M_w below 1000 g/mol (DP7) would gradually increase T_{onset}, while any fibre above that size did not show any further increase; which is in agreement with our findings. Above DP7, the temperature range of the gelatinization endotherm would significantly broaden compared to fibres with DP < 7. Hence, above 1000 g/mol additional mechanisms affects starch swelling and gelatinization, including size limiting, polydispersity and molecular structure (i.e. linear or branched). While the effect of $N_{OH,s}/v_s$ and of the hydrogen bond density $\Phi_{w,eff}$ of the solvent should be taken into account to explain the data obtained from (Kim & Setser, 1992) with DP < 7, a broadening of the melting transition could be clearly observed for M_w > 2000 g/mol in this study. In fact, two peaks appeared in 30% solutions with IQ (2184 g/mol) and TEX (3877 g/mol) (Fig. 8D), suggesting a change in the gelatinization mechanism compared to other sugar and sugar replacing solutions. However, the effect was observed depending on fibre concentration as also previously reported (Kim & Setser, 1992), with phase separation and the influence of the plasticizer on water structure likely to contribute (Renzetti et al., 2020). In presence of high M_w polysaccharides, the effective starch concentration in the continuous phase increases due to the different hydrodynamic volumes of the polymers (Gudmundsson, Eliasson, Bengtsson, & Aman, 1991) (Khanna & Tester, 2006), concentrating the starch in water cluster in presence of a concomitant fibre-rich phase. In such conditions, starch swelling and amylose leaching are inhibited, thus reducing peak viscosity (Bemiller, 2011; Qiu et al., 2015; Zhang et al., 2018; Hou et al., 2020). The effect becomes larger with increasing M_w of the soluble fibres (Qiu et al., 2016). Hence, it can be suggested that for soluble fibres with M_w > 2000 g/mol, less water is available to swell the granules due to phase separation and water retention by the fibres.

Based on the results of this study and the side chain liquid crystalline polymer model described by (Waigh et al., 2000; Donald, 2001), we propose the following interpretation of the effect of sugars and sugar replacers in the swelling and gelatinization behaviour of wheat starch (Fig. 10). The swelling behaviour (i.e. plasticization) of starch is controlled by an interplay of kinetic and thermodynamic factors related to solvent ingress and partitioning of plasticizers between solvent and starch, accounting for the G endotherm in the DSC traces (helix-helix dissociation). The kinetic factors are controlled by solvent viscosity and by the size of the plasticizers (sugars). The thermodynamic factors by the H-bonding ability of the plasticizers and by their partitioning between the two main phases (water and starch gel). Overall, these factors can be largely related to $N_{OH,s}/v_s$ and $\Phi_{w,eff}$, for sugars and sugar replacers up to about 2000 g/mol (Fig. 10), as pointed out earlier in the discussion. In conditions of excess H-bonding solvent, i.e. $\Phi_{w,eff}$>0.52 (based on evaluation of DSC traces obtained at different values of $\Phi_{w,eff}$) and of intermediate H-bonding solvent, i.e. 0.28≪$\Phi_{w,eff}$0.52, helix-helix dissociation is required before the helix-coil transition can occur. In such conditions, the kinetics factors become predominant with decreasing $N_{OH,s}/v_s$ (i.e. increasing M_w) of the plasticizer, thus resulting in a higher T_{onset} than what predicted from $\Phi_{w,eff}$ of the FH model. With further heating, the thermodynamic factors related to the melting of crystalline domains prevail (helix-coil transition), thus resulting in a good description of T_{peak} and T_{end} data by the FH model. Only in conditions of excess solvent with high sugar concentrations, T_{peak} may be still affected by the swelling kinetics, due to the merging of G and M endotherms. In conditions of limiting H-bonding solvent, i.e. $\Phi_{w,eff}$<0.28, a direct helix to coil phase change occurs from the crystalline state at elevated temperatures without an intermediate isotropic step (Waigh et al., 2000). Hence, the melting of the crystalline domains is mainly controlled by thermodynamics and $\Phi_{w,eff}$ can well describe T_{onset}, T_{peak} and T_{end}. For soluble fibres above the 2000 g/mol threshold, plasticizer ingress in the starch granule is limited while phase separation between a starch-rich and fibre-rich phase results in water partitioning between the two phases. As a result, swelling is mainly controlled by the availability of water, with an effective starch concentration in water clusters that increases with increasing M_w and concentration of the soluble fibres. As a result, the calculated $\Phi_{w,eff}$ does not reflect the environment around the starch granules and deviations from the FH model are observed at high concentrations of the large fibres in this study (i.e. 30% of TEX).

6. Conclusion

The palatability, structure and texture of cereal-based food is largely influenced by starch swelling and gelatinization behaviour. Understanding the mechanisms controlling these transformations in complex

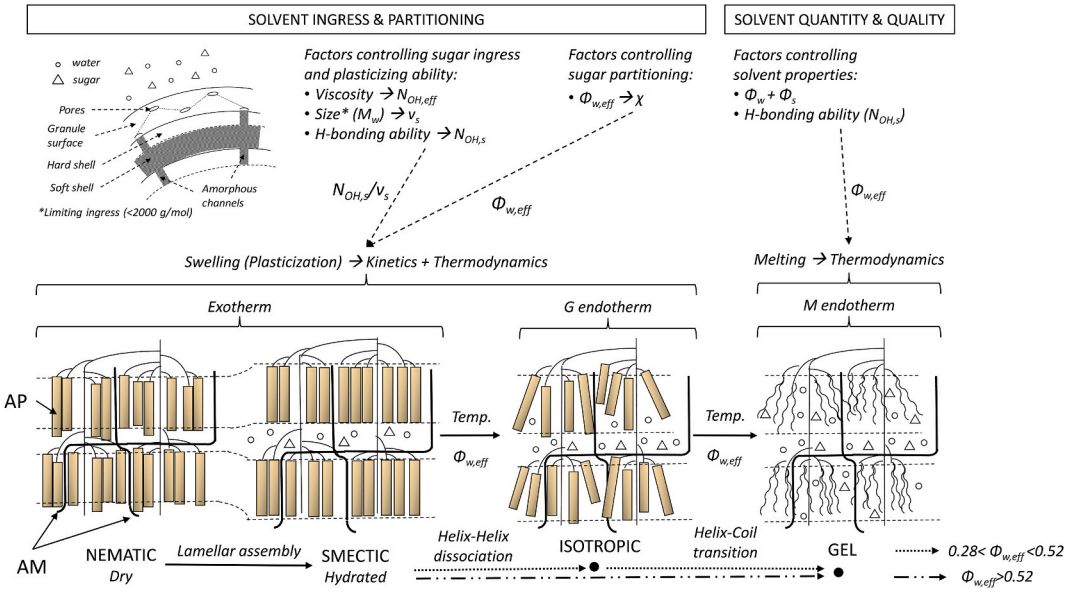

Fig. 10. Schematic description of factors controlling plasticization and gelatinization of A-type starch granule in presence of solvent under heating conditions. The representation is drawn from the results of this study based on the description of plasticization and self -assembly and gelatinization by (Waigh et al., 2000; Donald, 2001; Perry & Donald, 2002) and of the thermodynamics of starch swelling by (van Der Sman, 2018). AM is the amylose chains and AP is the amylopectin organized in double helices.

matrices is critical for designing food formulations towards improved nutritional composition, such as sugar reduction and fibre enrichment. In this study, evidence on the mechanisms by which sugars and sugar replacers modulate wheat starch gelatinization temperature and swelling (i.e. pasting) behaviour was provided. The T_{onset}, T_{peak} and T_{end} of starch gelatinization was shown to be a function of the effective solvent volume fraction $\Phi_{w,eff}$, which expresses the volume density of hydrogen bonding sites available in solution for interactions with starch. By applying the Flory-Huggins model for polymer melting extended with $\Phi_{w,eff}$, we have shown for the first time the ability to predict T_{onset}, T_{peak} and T_{end} in presence of different classes of compounds as well as mixtures thereof over a wide range of starch concentrations, covering conditions of limited, intermediate and excess solvent. Deviations from the FH model predictions were observed for T_{onset} in conditions of high sugar concentrations at intermediate and excess solvent, which are prone to phase separation into a starch-rich and a sugar-rich phase.

By concomitantly studying starch pasting behaviour, we showed for the first time that starch swelling (i.e. peak viscosity) in sugar and sugar replacers solutions is a sigmoidal function of $N_{OH,s}/v_s$for all concentrations tested (up to 40% w/w). The $N_{OH,s}/v_s$ is an intrinsic property of the plasticizer, which represents the number of H-bonding sites effectively available for intermolecular interactions within the molar volume of a sugar. Low $N_{OH,s}/v_s$ plasticizers (high M_w) showed decreased swelling with increasing concentration while the opposite occurred for high $N_{OH,s}/v_s$ plasticizers (low M_w). Taking together the results of gelatinization and pasting, we conclude that an interplay of kinetic factors (related to sugar ingress into the starch granule) and thermodynamics (related to sugar partitioning and plasticization ability of the solvent) control the swelling behaviour of starch associated with the side by side helix-helix dissociation (G endotherm). The kinetic factors can be largely related to $N_{OH,s}/v_s$ of the plasticizer, as it accounts for size as well as H-bonding ability of the plasticizer as well as for its contribution to the viscosity of the solution (van der Sman & Mauer, 2019; Renzetti et al., 2020). The thermodynamic factors are associated with $\Phi_{w,eff}$. With increasing M_w of the plasticizers, the interplay of kinetic factors and phase separation phenomena explain deviations of T_{onset} from the FH model at high concentrations of the plasticizers. In conditions of limited solvent, direct helix to coil transition (M endotherm) explain the good agreement between the FH model predictions and the observed T_{onset} for all studied solutions.

Overall, the result of this study combined with recent insights on the role of sugars and sugar replacers on food structuring processes (van der Sman & Renzetti, 2019; Renzetti et al., 2020; van der Sman & Renzetti, 2020), provide us with new avenues for more sophisticated and advanced reformulation approaches towards sugar reduction and fibre enrichment in cereal-based food.

CRediT authorship contribution statement

Stefano Renzetti: Conceptualization, Formal analysis, Visualization, Methodology, Writing – original draft, Writing – review & editing, Funding acquisition. **Irene A.F. van den Hoek:** Investigation, Data curation. **Ruud G.M. van der Sman:** Methodology, Writing – review & editing.

Declaration of competing interest

The authors declare that they have no known competing financial interests or personal relationships that could have appeared to influence the work reported in this paper.

Acknowledgements

This research was performed with additional funding from the Top Consortia for Knowledge and Innovation of the Dutch Ministry of Economic Affairs. Authors would like to thank Jolanda Henket and Eric Raaijmakers for their assistance in the sample preparation for DSC analysis and Eric Raaijmakers for the RVA experiments. Authors are thankful to Brigitte Peters (Sensus) for providing the oligofructoses used in the study (Frutalose OFP, Frutafit CLR, Frutafit IQ and Frutafit TEX).

Appendix A. Supplementary data

Supplementary data to this article can be found online at https://doi.org/10.1016/j.foodhyd.2021.106880.

References

Ahmad, F. B., & Williams, P. A. (1999). Effect of sugars on the thermal and rheological. *Biopolymers, 50*, 401–412.

Allan, M. C., Rajwa, B., & Mauer, L. J. (2018). Effects of sugars and sugar alcohols on the gelatinization temperature of wheat starch. *Food Hydrocolloids, 84*(June), 593–607. https://doi.org/10.1016/j.foodhyd.2018.06.035

Baek, M. H., Yoo, B., & Lim, S. (2004). Effects of sugars and sugar alcohols on thermal transition and cold stability of corn starch gel. *Food Hydrocollouds, 18*, 133–142. https://doi.org/10.1016/S0268-005X(03)00058-4

Bail, P. Le, Bizot, H., Ollivon, M., Keller, G., Bourgaux, C., & Bule, A. (1999). Monitoring the crystallization of amylose – lipid complexes during maize starch melting by synchrotron X-ray. *Biopolymes, 50*, 99–110.

Balet, S., Guelpa, A., Fox, G., & Manley, M. (2019). Rapid visco analyser (RVA) as a tool for measuring starch-related physiochemical properties in Cereals : A review. *Food Analytical Methods, 12*, 2344–2360. https://doi.org/10.1007/s12161-019-01581-w

Bemiller, J. N. (2011). Pasting , paste , and gel properties of starch – hydrocolloid combinations. *Carbohydrate Polymers, 86*(2), 386–423. https://doi.org/10.1016/j.carbpol.2011.05.064

Bertoft, E. (2018). Analyzing starch molecular structure. In S. Malin, & L. Nilsson (Eds.), *Starch in food. Structure, function and applications* (2nd ed., pp. 97–149). https://doi.org/10.1016/B978-0-08-100868-3.00002-0

Copeland, L., Blazek, J., Salman, H., & Tang, M. C. (2009). Food hydrocolloids form and functionality of starch. *Food Hydrocolloids, 23*(6), 1527–1534. https://doi.org/10.1016/j.foodhyd.2008.09.016

Donald, A. M. (2001). Plasticization and self assembly in the starch granule. *Cereal Chemistry, 78*(3), 307–314. https://doi.org/10.1094/CCHEM.2001.78.3.307

Donald, A. M. (2004). Understanding starch structure and functionality. In A.-C. Eliasson (Ed.), *Starch in food: Structure, function and applications* (pp. 156–184). Cambridge/Boca Raton: Woodhead Publishing Limited/CRC Press LLC.

Donald, A. M., Kato, K. L., Perry, P. A., & Waigh, T. A. (2001). Scattering studies of the internal structure of starch granules. *Starch - Stärke, 53*, 504–512.

Donovan, J. W. (1979). Phase transitions of the starch–water system. *Biopolymers, 18*(2), 263–275. https://doi.org/10.1002/bip.1979.360180204

Evans, I. D., & Haisman, D. R. (1982). The effect of solutes on the gelatinization temperature range of potato starch. *Starch - Stärke, 34*(7), 224–231. https://doi.org/10.1002/star.19820340704

Fox, T. G., & Flory, P. J. (1950). Second-Order Transition Temperatures and Related Properties of Polystyrene. I. Influence of Molecular Weight. *Journal of Applied Physics 21, 21*(6), 581. https://doi.org/10.1063/1.1699711

French, D. (1984). Organization of starch granules. In R. O. Y. WHISTLER, J. N. BEMILLER, & E. F. B. T. PASCHALL (Eds.), *Starch: Chemistry and technology* (2nd ed., pp. 183–247). Second. https://doi.org/10.1016/B978-0-12-746270-7.50013-6.

Gudmundsson, M., Eliasson, A., Bengtsson, S., & Aman, P. (1991). The effects of water soluble arabinoxylan on gelatinization and retrogradation of starch. *Starch - Stärke, 43*(1), S5–S10.

Hou, C., Zhao, X., Tian, M., Zhou, Y., Yang, R., Gu, Z., et al. (2020). Impact of water extractable arabinoxylan with different molecular weight on the gelatinization and retrogradation behavior of wheat starch. *Food Chemistry, 318*(February), 126477. https://doi.org/10.1016/j.foodchem.2020.126477

Jenkins, P. J., & Donald, A. M. (1998). Gelatinisation of starch: A combined SAXS/WAXS/DSC and sans study. *Carbohydrate Research, 308*(1–2), 133–147. https://doi.org/10.1016/S0008-6215(98)00079-2

Kawai, K., & Hagura, Y. (2012). Discontinuous and heterogeneous glass transition behavior of carbohydrate polymer-plasticizer systems. *Carbohydrate Polymers, 89*(3), 836–841. https://doi.org/10.1016/j.carbpol.2012.04.018

Khanna, S., & Tester, R. F. (2006). Influence of purified konjac glucomannan on the gelatinisation and retrogradation properties of maize and potato starches. *Food Hydrocolloids, 20*, 567–576. https://doi.org/10.1016/j.foodhyd.2005.05.004

Kim, S. S., & Setser, C. S. (1992). Kim 1992_Wheat starch gelatinization in the presence of polydextrose or hydrolyzed barley β-glucan.pdf. *Cereal Chemistry, 69*(4), 447–452.

Kovrlija, R., & Rondeau-Mouro, C. (2017). Hydrothermal changes in wheat starch monitored by two-dimensional NMR. *Food Chemistry, 214*, 412–422. https://doi.org/10.1016/j.foodchem.2016.07.051

Kugimiya, M., & Donovan, J. W. (1981). Calorimetric determination of the amylose content of starches based on formation and melting of the amylose-lysolecithin complex. *Journal of Food Science, 46*(3), 765–770. https://doi.org/10.1111/j.1365-2621.1981.tb15344.x

Kweon, M., Slade, L., & Levine, H. (2016a). Cake baking with alternative carbohydrates for potential sucrose replacement . I . Functionality of small sugars and their effects on high-ratio cake-baking performance. *Ceramic Transactions, 93*(6), 562–567.

Kweon, M., Slade, L., & Levine, H. (2016b). Cake baking with alternative carbohydrates for potential sucrose replacement . II . Functionality of healthful oligomers and their effects on high-ratio cake-baking performance. *Cereal Chemistry, 93*(6), 568–575.

Lerbret, A., Bordat, P., Affouard, F., Hédoux, A., Guinet, Y., & Descamps, M. (2007). How do trehalose, maltose, and sucrose influence some structural and dynamical properties of lysozyme? Insight from molecular dynamics simulations. *Journal of Physical Chemistry B, 111*(31), 9410–9420. https://doi.org/10.1021/jp071946z

Lim, H., Setser, C. S., & Paukstelis, J. V. (1992). Comparison of water mobility using 17O nuclear magnetic resonance for four: Glucose, maltose, maltotriose and sucrose. *Cereal Chemistry, 69*(4), 387–390.

Lins, R. D., Pereira, C. S., & Hünenberger, P. H. (2004). Trehalose-protein interaction in aqueous solution. *Proteins: Structure, Function, and Genetics, 55*(1), 177–186. https://doi.org/10.1002/prot.10632

Mensink, M. A., Frijlink, H. W., Van Der Voort Maarschalk, K., & Hinrichs, W. L. J. (2015). Inulin, a flexible oligosaccharide I: Review of its physicochemical characteristics. *Carbohydrate Polymers, 130*, 405–419. https://doi.org/10.1016/j.carbpol.2015.05.026

Miljkovic, M. (2010). Relative reactivity of hydroxyl groups in monosaccharides. In M. Miljković (Ed.), *Carbohydrates: Synthesis, mechanisms, and stereoelectronic effects* (pp. 113–142). New York, NY, USA: Springer. https://doi.org/10.1007/978-0-387-92265-2.

Nashed, G., & Sopade, P. A. (2003). The plasticisation effect of glycerol and water on the gelatinisation of wheat starch. *Starch - Stärke, 55*, 131–137.

Pawlus, S., Grzybowski, A., Paluch, M., & Wlodarczyk, P. (2012). Role of hydrogen bonds and molecular structure in relaxation dynamics of pentiol isomers. *Physical Review E, 85*, 1–4. https://doi.org/10.1103/PhysRevE.85.052501, 52501.

Pérez, S., Baldwin, P. M., & Gallant, D. J. (2009). Starch granules I. In *Starch: Chemistry and technology* (3rd ed., pp. 149–192). https://doi.org/10.1016/B978-0-12-746275-2.00005-7

Perry, P. A., & Donald, A. M. (2000). The role of plasticization in starch granule assembly. *Biomacromolecules, 1*, 424–432. https://doi.org/10.1021/bm0055145

Perry, P. A., & Donald, A. M. (2002). The effect of sugars on the gelatinisation of starch. *Carbohydrate Polymers, 49*(2), 155–165. https://doi.org/10.1016/S0144-8617(01)00324-1

Qiu, S., Yadav, M. P., Chen, H., Liu, Y., Tatsumi, E., & Yin, L. (2015). Effects of corn fiber gum (CFG) on the pasting and thermal behaviors of maize starch. *Carbohydrate Polymers, 115*, 246–252. https://doi.org/10.1016/j.carbpol.2014.08.071

Qiu, S., Yadav, M. P., Liu, Y., Chen, H., Tatsumi, E., & Yin, L. (2016). Food Hydrocolloids Effects of corn fi ber gum with different molecular weights on the gelatinization behaviors of corn and wheat starch. *Food Hydrocolloids, 53*, 180–186. https://doi.org/10.1016/j.foodhyd.2015.01.034

Renzetti, S., & Arendt, E. K. (2009). Effect of protease treatment on the baking quality of brown rice bread: From textural and rheological properties to biochemistry and microstructure. *Journal of Cereal Science, 50*(1). https://doi.org/10.1016/j.jcs.2009.02.002

Renzetti, S., Courtin, C. M., Delcour, J. A., & Arendt, E. K. (2010). Oxidative and proteolytic enzyme preparations as promising improvers for oat bread formulations: Rheological, biochemical and microstructural background. *Food Chemistry, 119*(4). https://doi.org/10.1016/j.foodchem.2009.09.028

Renzetti, S., van den Hoek, I. A. F., & van der Sman, R. G. M. (2020). Amino acids , polyols and soluble fibres as sugar replacers in bakery applications : Egg white proteins denaturation controlled by hydrogen bond density of solutions. *Food Hydrocolloids, 108*(May), 106034. https://doi.org/10.1016/j.foodhyd.2020.106034

Roudaut, G., & Wallecan, J. (2015). New insights on the thermal analysis of low moisture composite foods. *Carbohydrate Polymers, 115*, 10–15. https://doi.org/10.1016/j.carbpol.2014.08.066

Slade, L., & Levine, H. (1988). Non-equilibrium melting of native granular Starch : Part I . Temperature location of the glass transition associated with gelatinization of A-type cereal starches. *Carbohydrate Polymers, 8*, 183–208.

van der Sman, R. G. M. (2016). Sugar and polyol solutions as effective solvent for biopolymers. *Food Hydrocolloids, 56*, 144–149. https://doi.org/10.1016/j.foodhyd.2015.12.001

van der Sman, R. G. M. (2019). Phase separation, antiplasticization and moisture sorption in ternary systems containing polysaccharides and polyols. *Food Hydrocolloids, 87*(July 2018), 360–370. https://doi.org/10.1016/j.foodhyd.2018.07.051

van der Sman, R. G. M., & Mauer, L. J. (2019). Starch gelatinization temperature in sugar and polyol solutions explained by hydrogen bond density. *Food Hydrocolloids, 94*, 371–380. https://doi.org/10.1016/j.foodhyd.2019.03.034

van der Sman, R. G. M., & Renzetti, S. (2019). Understanding functionality of sucrose in biscuits for reformulation purposes. *Critical Reviews in Food Science and Nutrition, 59*(14), 2225–2239. https://doi.org/10.1080/10408398.2018.1442315

van der Sman, R. G. M., & Renzetti, S. (2020). Understanding functionality of sucrose in cake for reformulation purposes. *Critical Reviews in Food Science and Nutrition*, 1–17. https://doi.org/10.1080/10408398.2020.1786003

van der Sman, R. G. M., van den Hoek, I. A. F., & Renzetti, S. (2020). Sugar replacement with zwitterionic plasticizers like amino acids. *Food Hydrocolloids, 109*(May), 106113. https://doi.org/10.1016/j.foodhyd.2020.106113

Spies, R. D., & Hoseney, R. C. (1982). Effect of sugars on starch gelatinization. *Cereal Chemistry, 59*(2), 128–131.

Steeneken, P. A. M., & Woortman, A. J. J. (2009). Identification of the thermal transitions in potato starch at a low water content as studied by preparative DSC. *Carbohydrate Polymers, 77*(2), 288–292. https://doi.org/10.1016/j.carbpol.2008.12.026

Svensson, E., & Eliasson, A. (1995). Crystalline changes in native wheat and potato starches at intermediate water levels during gelatinization. *Carbohydrate Polymers, 26*, 171–176.

Tananuwong, K., & Reid, D. S. (2004). DSC and NMR relaxation studies of starch – water interactions during gelatinization. *Carbohydrate Polymers, 58*, 345–358. https://doi.org/10.1016/j.carbpol.2004.08.003

Tan, I., Wee, C. C., Sopade, P. A., & Halley, P. J. (2004). Investigation of the starch gelatinisation phenomena in water – glycerol systems : Application of modulated temperature differential scanning calorimetry. *Carbohydrate Polymers, 58*, 191–204. https://doi.org/10.1016/j.carbpol.2004.06.038

Tester, R. F., Karkalas, J., & Qi, X. (2004). Starch - composition, fine structure and architecture. *Journal of Cereal Science, 39*(2), 151–165. https://doi.org/10.1016/j.jcs.2003.12.001

Tester, R. F., & Sommerville, M. D. (2003). The effects of non-starch polysaccharides on the extent of gelatinisation , swelling and a -amylase hydrolysis of maize and wheat starches. *Food Hydrocolloids, 17*, 41–54.

Ubbink, J. (2016). Structural and thermodynamic aspects of plasticization and antiplasticization in glassy encapsulation and biostabilization matrices. *Advanced Drug Delivery Reviews, 100*, 10–26. https://doi.org/10.1016/j.addr.2015.12.019

Van Der Sman, R. G. M., & Meinders, M. B. J. (2011). Prediction of the state diagram of starch water mixtures using the Flory-Huggins free volume theory. *Soft Matter, 7*(2), 429–442. https://doi.org/10.1039/c0sm00280a

van der Sman, R. G. M. (2013). Predictions of glass transition temperature for hydrogen bonding biomaterials. *Journal of Physical Chemistry B, 117*(50), 16303–16313. https://doi.org/10.1021/jp408184u

van Der Sman, R. G. M. (2018). Theoretical investigation of the swelling of polysaccharide microgels in sugar solutions. *Food and Function, 9*(5), 2716–2724. https://doi.org/10.1039/c8fo00452h

Waigh, T. A., Gidley, M. J., Komanshek, B. U., & Donald, A. M. (2000). The phase transformations in starch during gelatinisation: A liquid crystalline approach. *Carbohydrate Research, 328*(2), 165–176. https://doi.org/10.1016/S0008-6215(00)00098-7

Wang, S., Li, C., Yu, J., Copeland, L., & Wang, S. (2014). LWT - food Science and Technology Phase transition and swelling behaviour of different starch granules over a wide range of water content. *Lebensmittel-Wissenschaft und -Technologie- Food Science and Technology, 59*(2), 597–604. https://doi.org/10.1016/j.lwt.2014.06.028

Wang, S., Zhang, X., Wang, S., & Copeland, L. (2016). Changes of multi-scale structure during mimicked DSC heating reveal the nature of starch gelatinization. *Nature Scientific Reports*, (March), 1–9. https://doi.org/10.1038/srep28271

Yuryev, V. P., Nemirovskaya, I. E., & Maslova, T. D. (1995). Phase state of starch gels at different water contents. *Carbohydrate Polymers, 26*, 43–46.

Zhang, B., Bai, B., Pan, Y., Li, X., Cheng, J., & Chen, H. (2018). Effects of pectin with different molecular weight on gelatinization behavior, textural properties, retrogradation and in vitro digestibility of corn starch. *Food Chemistry, 264*(May), 58–63. https://doi.org/10.1016/j.foodchem.2018.05.011